Check for updates

View Article Online
View Journal

Food & Function

Linking the chemistry and physics of food with health and nutrition

Accepted Manuscript

This article can be cited before page numbers have been issued, to do this please use: A. L. Dordevic, M. Murray, M. J. Houghton, N. M. Trinquet, N. J. Kellow, R. B. Schittenhelm, C. K. Barlow, K. Day, L. Bennett, B. Colton and G. Williamson, *Food Funct.*, 2026, DOI: 10.1039/D5FO04456A.

This is an Accepted Manuscript, which has been through the Royal Society of Chemistry peer review process and has been accepted for publication.

Accepted Manuscripts are published online shortly after acceptance, before technical editing, formatting and proof reading. Using this free service, authors can make their results available to the community, in citable form, before we publish the edited article. We will replace this Accepted Manuscript with the edited and formatted Advance Article as soon as it is available.

You can find more information about Accepted Manuscripts in the Information for Authors.

Please note that technical editing may introduce minor changes to the text and/or graphics, which may alter content. The journal's standard Terms & Conditions and the Ethical guidelines still apply. In no event shall the Royal Society of Chemistry be held responsible for any errors or omissions in this Accepted Manuscript or any consequences arising from the use of any information it contains.

ROYAL SOCIETY OF CHEMISTRY

rsc.li/food-function

View Article Online
DOI: 10.1039/D5FO04456A

Acute response to a high-saturated-fat, high-refined carbohydrate meal in healthy young men shows novel perturbation of multiple metabolic and defense pathways

Aimee L Dordevic [1, 2] aimee.dordevic@monash.edu, ORCID 0000-0002-0405-3164

Margaret Murray [1, 3, 4] msmurray@swin.edu.au, ORCID 0000-0003-3767-6947

Michael J Houghton [1,2] michael.houghton@monash.edu, ORCID 0000-0001-6579-7995

Nina M Trinquet [1,2] nina.trinquet1@monash.edu, ORCID 0009-0009-2828-2963

Nicole J Kellow [1,2] nicole.kellow@monash.edu, ORCID 0000-0002-4511-7259

Ralf B Schittenhelm [5] ralf.schittenhelm@monash.edu, ORCID 0000-0001-8738-1878

Christopher K Barlow [5] chris.barlow@monash.edu, ORCID 0000-0001-9309-2829

Kaitlin Day [6] kaitlin.day@kcl.ac.uk, ORCID 0000-0003-3846-8568

Louise Bennett [3] louise.bennett1@monash.edu, ORCID 0000-0001-9421-4410

Beau-Luke Colton [1] beau.colton@gmail.com

Gary Williamson [1,2,7] g.williamson@qub.ac.uk, ORCID 0000-0002-5624-6267

[1]Department of Nutrition, Dietetics & Food, Monash University, Notting Hill, Victoria, 3168, Australia

[2]Victorian Heart Institute, Monash University, Clayton, Victoria, 3168, Australia

[3]School of Chemistry, Monash University, Clayton, Victoria, 3800, Australia

[4]Department of Biomedical, Health and Exercise Sciences, Swinburne University of Technology, Hawthorn, Victoria, 3122, Australia

[5]Monash Proteomics & Metabolomics Platform, Monash Biomedicine Discovery Institute & Department of Biochemistry and Molecular Biology, Monash University, Clayton VIC 3800, Australia

Open Access Article. Published on 31 March 2026. Downloaded on 4/2/2026 12:19:51 AM.
This article is licensed under a Creative Commons Attribution 3.0 Unported Licence.

Food & Function Accepted Manuscript

View Article Online
DOI: 10.1039/D5FO04456A

[6]Department of Nutritional Sciences, Faculty of Life Sciences and Medicine, Kings College London

[7]School of Biological Sciences, Queen's University, Belfast, BT7 1NN, UK

Corresponding author: Dr Gary Williamson, School of Biological Sciences, Queen's University, Belfast, BT7 1NN, UK

g.williamson@qub.ac.uk

Registration ID ACTRN12619000929101

https://www.anzctr.org.au/Trial/Registration/TrialReview.aspx?id=377814&isReview=true

Funding: Monash University

Open Access Article. Published on 31 March 2026. Downloaded on 4/2/2026 12:19:51 AM.
This article is licensed under a Creative Commons Attribution 3.0 Unported Licence.

Food & Function Accepted Manuscript

View Article Online
DOI: 10.1039/D5FO04456A

Open Access Article. Published on 31 March 2026. Downloaded on 4/2/2026 12:19:51 AM.
This article is licensed under a Creative Commons Attribution 3.0 Unported Licence.

Food & Function Accepted Manuscript

Abstract

Background: Metabolic flexibility is characterized by a complex response in blood markers rapidly returning to baseline after a high-saturated-fat, high-refined-carbohydrate meal, and this adaptability is progressively lost as chronic metabolic dysfunction develops.

Objective: To comprehensively profile the postprandial response and identify novel potential biomarkers related to defense, oxidative stress and other processes, to better define metabolic flexibility.

Methods: Conventional methods as well as metabolomics and proteomics were used to profile the response in 12 healthy men to a high-saturated-fat, high-refined-carbohydrate meal, at hourly time points both before and after consumption.

Results: In addition to the expected changes in glucose, insulin, triglycerides, fatty acids and myeloperoxidase, we observed multiple previously unreported changes in the plasma proteome, including a compromised "cellular oxidant detoxification" pathway (55 proteins) at 4 and 5 hours after the meal. Between individuals, the magnitude of the decrease in Cu-Zn-superoxide dismutase protein was associated with plasma postprandial glucose area-under-the-curve ($r = -0.767$, $p = 0.004$). In contrast, the peripheral blood mononuclear cell proteome showed minimal changes over 6 hours. Through plasma metabolomic analysis, we observed many novel postprandial changes with potential use as biomarkers, most notably increases in oxidative stress-related products such as myeloperoxidase putative products L-methionine S-oxide, 3-(4-hydroxyphenyl)pyruvate, and L-homocitrulline and in gut microbiota metabolites such as hydroxy-isocaproic acid, as well as a sustained elevation of phenylalanine, tyrosine, and branched chain amino acids at 6 hours.

Conclusion: These data indicate a complex diminution of plasma defense proteins after a high-saturated fat high-refined carbohydrate meal, and then a return to baseline reflecting metabolic

View Article Online
DOI: 10.1039/D3FO04456A

flexibility in the cohort of healthy young men. However, the data also show that some risk markers and stress products are still elevated 6 hours after the meal. The data provide a valuable resource for future postprandial metabolomic studies assessing the protective effect of nutrients and phytochemicals on postprandial stresses, and enabling comparisons between healthy and compromised populations. Trial Registration: ACTRN12619000929101.

Keywords: postprandial, proteomics, metabolomics, oxidative stress, myeloperoxidase, superoxide dismutase

Open Access Article. Published on 31 March 2026. Downloaded on 4/2/2026 12:19:51 AM.
This article is licensed under a Creative Commons Attribution 3.0 Unported Licence.

Food & Function Accepted Manuscript

View Article Online
DOI: 10.1039/D5FO04456A

Open Access Article. Published on 31 March 2026. Downloaded on 4/2/2026 12:19:51 AM.
This article is licensed under a Creative Commons Attribution 3.0 Unported Licence.

Food & Function Accepted Manuscript

Abbreviation list

AAC, area above the curve

ANOVA, analysis of variance

AUC, area under the curve

BMI, body mass index

EDTA, ethylenediamine tetraacetic acid

ELISA, enzyme-linked immunosorbent assay

FDR, false discovery rate

GC, gas chromatography

HFHCM, high-saturated-fat, high-refined-carbohydrate meal

HPAEC-PAD, high-performance anion-exchange chromatography with pulsed amperometric detection

IL, interleukin

MPO, myeloperoxidase

MUFA, monounsaturated fatty acid

PBMC, peripheral blood mononuclear cell

PBS, phosphate buffered saline

PUFA, polyunsaturated fatty acid

RCF, relative centrifugal force

SD, standard deviation

SOD, superoxide dismutase

WBC, white blood cell

View Article Online
DOI: 10.1039/D5FO04456A

Open Access Article. Published on 31 March 2026. Downloaded on 4/2/2026 12:19:51 AM.
This article is licensed under a Creative Commons Attribution 3.0 Unported Licence.

Food & Function Accepted Manuscript

Introduction

Habitual consumption of energy-dense, nutrient poor foods that are high in saturated fat and refined carbohydrates, leads to increased risk of cardiovascular diseases, obesity, immune dysfunction and type 2 diabetes (1-4). The metabolic response to a high-saturated-fat, high-refined-carbohydrate meal (HFHCM) includes blood glucose spikes, increases in total plasma triglycerides and increases in insulin. All are well characterized and the magnitudes of these responses are clearly dependent on health status, and have been used to diagnose metabolic inflexibility, with insulin sensitivity and the gut microbiota composition playing an important role in differences between individuals (5, 6). However, it is becoming increasingly recognized that the biological response to a HFHCM is much more complex than indicated from measurement of postprandial glucose and lipid levels alone. Plasma metabolomics focusing on changes in total fatty acids, triglycerides, amino acids and canonical pathway intermediates have been reported in response to various meals and in various population groups (7-10), yet comprehensive time-dependent global plasma protein changes using proteomics are unexplored despite the importance of plasma proteins in cellular and whole body defenses.

One of the proposed biological responses to a HFHCM is oxidative stress, which ultimately leads to chronic disease through inflammatory processes (11-14). Postprandial oxidative stress is evidenced by transient increases in lipid hydroperoxides (15, 16), oxidized low density lipoprotein (17, 18), malondialdehyde (19, 20), and myeloperoxidase (MPO) (21, 22). In addition, a HFHCM induces an influx of macronutrients into tissues including skeletal muscle, liver, adipose and vascular endothelial cells. Elevated cellular metabolism of glucose and fatty acids can generate reactive oxygen species (ROS), which are reduced by endogenous antioxidant enzymes such as mitochondrial and cytosolic superoxide dismutases (SOD) (23). Hyperglycemia-induced superoxide over-production inhibits the glycolytic enzyme

View Article Online
DOI: 10.1039/D5FO04456A

Open Access Article. Published on 31 March 2026. Downloaded on 4/2/2026 12:19:51 AM.
This article is licensed under a Creative Commons Attribution 3.0 Unported Licence.

Food & Function Accepted Manuscript

glyceraldehyde-3-phosphate dehydrogenase in endothelial cells (24) resulting in diversion of accumulated glycolytic intermediates through alternative pathways (25) including the polyol pathway, activation of protein kinase-C, and formation of advanced glycation end products, which are all known to mediate tissue damage (26). Proteins in the blood are secreted from, and taken up by, various organs, including the liver and intestine, but also from peripheral blood mononuclear cells (PBMC) and the vascular endothelium, and so transient changes are expected in response to a meal. Indeed, several very low abundance proteins are classically known to increase in response to food such as insulin and incretin hormones, and also some specific proteins such as MPO as described above (21, 27-29).

We hypothesized that a HFHCM would induce multiple postprandial metabolites and protein markers of stress in addition to classical markers. While conventional markers such as glucose and insulin have been extensively measured in postprandial studies, markers of potential damage after a HFHCM have not been addressed at the proteome level, nor associated changes in the metabolome. We have addressed this gap by studying the effects of a well-characterized HFHCM on multiple blood parameters in metabolically competent individuals and suggest several biomarkers of postprandial metabolic stress. We have also provided a resource that can be used for future studies including a listing of multiple as yet unknown metabolites that change after a meal.

View Article Online
DOI: 10.1039/D5FO04456A

Open Access Article. Published on 31 March 2026. Downloaded on 4/2/2026 12:19:51 AM.
This article is licensed under a Creative Commons Attribution 3.0 Unported Licence.

Food & Function Accepted Manuscript

Methods

Trial design

This trial was a control and experimental two-phase single-arm study, registered with the Australian and New Zealand Clinical Trials Register (ANZCTR) (Trial ID: ACTRN12619000929101). The Monash University Human Research Ethics Committee approved all experimental procedures (2019-18917-32133), which were in accordance with the Declaration of Helsinki. All participants in this study gave their written informed consent to participate.

Participants and study procedure

Healthy males aged 18 to 35 years were recruited via flyers on campus, social media (Facebook, Twitter and Instagram) and university department websites; eligible applicants were not taking medications or supplements with antioxidant activity, or anything that might have affected metabolism or nutrient absorption; were not diagnosed with a medical condition; did not consume more than 14 standard drinks of alcohol per week; had a body mass index (BMI) from 18.5 to 29.9 kg/m^2 (> 25 kg/m^2, n = 2); had blood pressure between 90/60 to 140/90 mmHg; did not smoke; did not have an implanted cardiac defibrillator; and did not have any known dietary requirements that prevented them from consuming the study meals. Male volunteers were selected to prevent variance in results that may arise from hormonal fluctuations associated with the menstrual cycle (30). Participants completed an online screening survey to determine initial eligibility, and eligible participants were invited to attend a screening visit at the university research facility during which anthropometric measurements (height, weight, waist circumference, BMI, body composition) were collected, and blood pressure was measured to assess whether participants met the inclusion criteria.

View Article Online
DOI: 10.1039/D3FO04456A

Open Access Article. Published on 31 March 2026. Downloaded on 4/2/2026 12:19:51 AM.
This article is licensed under a Creative Commons Attribution 3.0 Unported Licence.

Food & Function Accepted Manuscript

The night before the testing visit, volunteers consumed a standard, commercial dinner meal (McCain Man Size Chicken & Bacon Bake: 43.2 g protein, 33.6 g fat (21.6 g saturated), 74.9 g carbohydrate (3.4 g sugar), 1440 mg sodium, 3290 kJ (787 kcal)) between 7 and 9 pm then fasted overnight. For 24-hours prior to testing, participants were asked to avoid strenuous exercise.

Fasting control phase

Upon arrival at 8:00 am, participants had an intravenous cannula inserted and three fasting venous blood samples taken, 1 hour apart (-120, -60, 0 min). This two-hour run-in period, prior to the HFHCM, was to determine any changes in biomarkers before the meal and serve as a control. A fasting capillary blood sample was taken via finger prick, one hour prior to the HFHCM.

Postprandial experimental phase

After blood collection at 0 min, participants were given 15 min to consume the HFHCM, following which venous blood samples were taken every 15 min for the first hour, then every 30 min for the next two hours and then every 60 min for the remaining three hours, up to six hours (360 min) post-meal consumption. Finger prick capillary blood samples were taken at 60 and 120 min after the HFHCM. Following the HFHCM, participants did not consume any additional food until the end of the study period, but were allowed water *ad libitum*. Capillary blood samples were used to measure WBC counts, and the venous blood samples were used to measure all other biomarkers.

View Article Online
DOI: 10.1039/D5FO04456A

Open Access Article. Published on 31 March 2026. Downloaded on 4/2/2026 12:19:51 AM.
This article is licensed under a Creative Commons Attribution 3.0 Unported Licence.

Food & Function Accepted Manuscript

Composition and analysis of the HFHCM

The HFHCM contained 40 g refined coconut oil (Pure, SSM Brand, International), 10 g animal fat (Supafry, Goodman Fielder, Australia), 30 g castor sugar (sucrose) (Sugar Australia, Australia), 25 g maltodextrin (100%, Bulk Foods, Tasmania, Australia), 170 g skim milk powder (Devondale, Australia), 175 g full cream long life milk (Devondale, Australia), 52 g thickened cream (Bulla, Victoria, Australia) and 15 g of water. The ingredients were adjusted for each participant according to participant weight divided by 70 kg (the standard measures were based on a 70 kg adult), with the exception of the volume of water that remained constant (15 g).

Proximate analysis (ash (as is), fat by acid hydrolysis, fatty acid profile, oven moisture, and Kjeldahl), and amino acid analyses were performed by Agrifood Technology Pty Ltd (Werribee VIC, Australia). For amino acids, samples underwent hydrolysis in 6 M HCl at 110 ^{0}C, then labelled using the AccQTag Ultra chemistry kit (Waters, Rydalmere NSW) according to the supplier's recommendations, and analyzed on a Waters Acquity UPLC. Using this method, asparagine is hydrolyzed to aspartic acid, and glutamine to glutamic acid, therefore the reported amounts are the sums of the respective components; and cysteine and tryptophan are not analyzed by this method. All samples were analyzed in duplicate. Fatty acids were analyzed by gas chromatography (GC). To each sample, ten drops of 2M KOH in methanol were added, mixed, and then 1 ml of hexane added. The vial was sealed and placed in a water bath at 50 ^{0}C with vigorous mixing every 10-20 seconds for 3 min. Sample was then removed from the bath and allowed to stand for 1 min to separate the phases. The hexane phase (0.5 µL) was injected into the GC. Analysis was performed on an Agilent 7820A GC with manual syringe injection of 0.5 µL of sample, and the inlet split set to 10:1. The column was a Supelco Wax capillary 30 m x 320 um, with film thickness 0.25 um, with nitrogen as the carrier gas running at 1.1

View Article Online
DOI: 10.1039/D5FO04456A

ml/min. The oven temperature program was held initially at 90 ^{0}C for 1 min, then increased by 15 ^{0}C /min to 245 ^{0}C and held for 2.5 min. Detection was by flame ionization set at 300 ^{0}C. Sugar analysis was performed using high-performance anion-exchange chromatography with pulsed amperometric detection [HPAEC-PAD) ion chromatography (see method below).

Anthropometric and blood pressure measurements

Height was measured using a Harpenden Stadiometer (Holtain, Crymych) with participants' shoes and socks removed. Weight, visceral fat and total body fat were measured by bioelectrical impedance analysis using a medical body composition analyzer (Ecomed, Seven Hills, NSW, Australia) with shoes and socks removed and participants in light clothing. Blood pressure was measured in duplicate with the participant in a relaxed, seated position using a portable sphygmomanometer (WelchAllyn, Skaneateles Falls, New York, USA) and the results averaged.

Sample collection and preparation

Venous blood samples for serum were collected into BD Vacutainer® SSTTM II Advance tubes (North Ryde, New South Wales, Australia), allowed to clot for 30 min, centrifuged at 2.0 relative centrifugal force (RCF) for 5 min at 22-25°C and stored at -80°C until analysis. Venous blood samples for plasma were collected into BD Vacutainer® K2EDTA Tubes (North Ryde, New South Wales, Australia) and immediately centrifuged at 1.5 RCF for 10 min at 4°C and stored at -80°C until analysis. Plasma aliquots had 20 µL of ethylenediamine tetraacetic acid (EDTA) (0.1% w/v) and ascorbic acid (20% w/v) added per 500 µL, and then were stored at -80°C. PBMCs, for proteomic analysis, were collected in BD Vacutainer® CPT™ System Tubes (North Ryde, New South Wales, Australia) at fasting, 180 and 360 min after the HFHCM, and immediately centrifuged at 1.5 RCF for 25 minutes at 22°C with the brake off.

Open Access Article. Published on 31 March 2026. Downloaded on 4/2/2026 12:19:51 AM.
This article is licensed under a Creative Commons Attribution 3.0 Unported Licence.

Food & Function Accepted Manuscript

View Article Online
DOI: 10.1039/D5FO04456A

Open Access Article. Published on 31 March 2026. Downloaded on 4/2/2026 12:19:51 AM.
This article is licensed under a Creative Commons Attribution 3.0 Unported Licence.

Food & Function Accepted Manuscript

The mononuclear and platelet cell layer was transferred to a 15 mL falcon tube and topped up to 10 mL with phosphate-buffered saline (PBS), then centrifuged at 1.0 RCF for 15 minutes at 22°C with the brake on. After the excess supernatant was discarded, the cell pellet was resuspended in the remaining amount of supernatant, transferred to a 1.7 mL Eppendorf tube and centrifuged a final time at 1.0 RCF for 15 minutes at 22°C. Any remaining PBS was removed, the residual cells were snap frozen in liquid nitrogen and stored at -80°C. All venous blood samples were stored in cryogenic-safe Eppendorf tubes.

Measurement of serum myeloperoxidase (MPO)

We estimated MPO activity *in vivo* by measuring MPO-generated products in the blood through metabolomic analysis and additionally measured MPO protein using the human myeloperoxidase enzyme-linked immunosorbent assay (ELISA) kit (ab119605) from Abcam (Cambridge, UK), following the manufacturer's guidelines. Absorbance was measured at 450 nm using a PHERAstar FS plate reader. Intra- and inter-assay precision for the MPO ELISA was 8.8% and 9.9%, respectively, close to the manufacturer's guidelines.

Measurement of plasma superoxide dismutase 1 protein

SOD1 was quantified in plasma samples using the Invitrogen Human Cu/ZnSOD ELISA kit from Thermo Fisher Scientific, following manufacturer's guidelines. Plasma samples were analyzed in triplicate, and the absorbance was measured at 450 nm using PHERAstar FS plate reader. Intra- and inter-assay precision for the SOD1 ELISA were 4.7% and 5.5%, respectively, both within the acceptable range (5.1% and 5.8%, respectively).

View Article Online
DOI: 10.1039/D5FO04456A

Open Access Article. Published on 31 March 2026. Downloaded on 4/2/2026 12:19:51 AM.
This article is licensed under a Creative Commons Attribution 3.0 Unported Licence.

Food & Function Accepted Manuscript

Measurement of plasma white blood cells

Blood samples for WBC count were taken by capillary finger prick on the index, middle and ring fingers of each hand using a new finger at each time point to eliminate measurement of any inflammatory response from the previous injury. Samples were taken from one finger on each hand (cannulated and non-cannulated arm) at each time point. After sterilization of the fingertip, blood was drawn using a disposable lancet. The first 3 drops of blood were wiped with a cotton ball and discarded. A micro cuvette was filled with the blood sample and inserted into a HemoCue WBC DIFF analyzer (Radiometer, Pacific), which displayed the total count for WBC, neutrophils, lymphocytes, monocytes, eosinophils and basophils (31). Cell counts did not differ between the cannulated and non-cannulated arm samples, and results are presented as an average of the replicate measurements.

Measurement of plasma glucose and serum triglycerides

Plasma triglyceride and glucose concentrations were measured on a Thermo Fisher Indiko clinical chemistry analyzer (Thermo Fisher Scientific, Vantaa, Finland) by enzymatic colorimetric methods using commercially available kits according to the manufacturer's instructions (Thermo Fisher Scientific, Vantaa, Finland).

Measurement of plasma insulin

Serum insulin was measured using the Millipore ELISA Kits for human insulin (Cat. # EZHI-14K, Merck Millipore, Bayswater, Australia), according to kit instructions. Each sample was assessed in triplicate and absorbance was measured using the SPECTROstar Nano microplate reader (450 nm wavelength, BMG Labtech, Mornington, Australia). The lowest level of insulin (LOD, limit of detection) detectable by this assay is 1 μU/mL, and so all samples with

View Article Online
DOI: 10.1039/D5FO04456A

Open Access Article. Published on 31 March 2026. Downloaded on 4/2/2026 12:19:51 AM.
This article is licensed under a Creative Commons Attribution 3.0 Unported Licence.

Food & Function Accepted Manuscript

280 undetectable insulin were assigned this value. The units were converted from µU/mL to pmol/L
281 using the conversion factor of 6 (32) prior to statistical analysis. Intra- and inter-assay precision
282 for the insulin ELISA were 8.1% and 6.7%, respectively.
283
284 *Plasma metabolomics analysis*
285 Samples used for metabolomic analyses were all fasting time points (-120, -60, 0 min), and
286 postprandial time points 60, 120, and 360 min. Plasma was thawed on ice before adding 25 µL
287 to 200 µL of ice-cold extraction solvent (1:1 acetonitrile:methanol v/v, internal standards: 2
288 µM CHAPS, CAPS, PIPES and TRIS), followed by vortex mixing for 30 minutes at 4°C before
289 centrifugation (20,000 ×g, 4°C, 15 minutes). The supernatant was then immediately analyzed.
290 A Dionex RSLC3000 UHPLC coupled to a Q-Exactive Plus Orbitrap MS (Thermo) was used
291 for untargeted metabolomic analysis (33), using a ZIC-p(HILIC) column (5 µm, 150 x 4.6 mm)
292 with a ZIC-pHILIC guard column (20 x 2.1 mm) (both Merck Millipore, Australia). A gradient
293 elution of 20 mM ammonium carbonate (A) and acetonitrile (B) (linear gradient time-%B: 0
294 min-80%, 15 min-50%, 18 min-5%, 21 min-5%, 24 min-80%, 32 min-80%) was utilized at 25
295 °C, with 300 µL/min flow rate. Samples were kept cooled at 6°C until 10 µL was injected. MS
296 was performed at 35,000 resolution operating in rapid switching positive (4 kV) and negative
297 (−3.5 kV) mode electrospray ionization (capillary temperature 300°C; sheath gas flow rate 50;
298 auxiliary gas flow rate 20; sweep gas 2; probe temp 120°C). A library of ~350 metabolite
299 standards were analyzed alongside the samples to facilitate metabolite identification and
300 formed the basis of a retention time prediction model used to provide putative identification of
301 metabolites not contained within the standard library (34). Acquired LC-MS/MS data were
302 processed in an untargeted fashion using the open source software IDEOM, which initially
303 used msConvert (ProteoWizard) (35) to convert raw LC-MS files to mzXML format, and
304 XCMS to select peaks to convert to .peakML files (36). Mzmatch was subsequently used for

View Article Online
DOI: 10.1039/D5FO04456A

305 sample alignment and filtering (37), and IDEOM was utilized for further data pre-processing,
306 organization and quality evaluation (36).

307

308 Using relative peak intensities, missing, or zero values were replaced by 20% of the minimum
309 positive values of their corresponding variables. Fold changes were calculated and log2
310 transformed. Peak intensities were then normalized using log10-transformation for statistical
311 analysis. Pre-processing was performed in MetaboAnalyst (5.0: metaboanalyst.ca/home), and
312 ANOVA was performed in R statistical analysis software (version 4.2.2). To assess changes
313 over time, a one-way ANOVA was performed with FDR adjustment for multiple comparisons,
314 and for significant results, a Tukey post-hoc test was performed for comparisons of each time
315 point with 0 min. Metabolites that were significantly changed at one of the postprandial time
316 points (adjusted p-value < 0.01) and not changed during the control period were assessed. The
317 identified compounds were manually sorted into classes, and were considered as confirmed if
318 their mass and retention time matched standards from the in-house library.

319

320 *Quantification of sugars in the meal and in plasma by HPAE-PAD ion chromatography*
321 The Dionex Integrion High Performance Ion Chromatography system was used for HPAE-
322 PAD (Thermo Fisher Scientific Inc., Waltham, MA, USA) for the separation and analysis of
323 sugars in plasma, and the HFHCM diluted in water, with prepared sugar standards and plasma
324 or meal samples undergoing the same relative treatment prior to injection (38). All were
325 deproteinated by mixing with an equal volume of acetonitrile, vortexed for 30 s and centrifuged
326 at 17,000 × g, 15 min at 4°C. The resulting supernatants were then diluted in water (maximum
327 final acetonitrile concentration 5% (v/v)) and kept at 8°C on the autosampler before injection
328 (2.5 µL, in duplicate). A CarboPac PA210 column at 30°C (2 × 150 mm), preceded by a
329 CarboPac PA210 Guard column at 20°C (2 × 30 mm), was used. Eluent was generated using

Open Access Article. Published on 31 March 2026. Downloaded on 4/2/2026 12:19:51 AM.
This article is licensed under a Creative Commons Attribution 3.0 Unported Licence.

Food & Function Accepted Manuscript

View Article Online
DOI: 10.1039/D5FO04456A

a Dionex EGC 500 KOH eluent generator cartridge with continuously regenerated-anion trap column 600, as follows: 12 mM for 12 minutes, 100 mM for 8 minutes and 12 mM for 12 minutes, at a flow rate of 0.2 mL/min. Detection used a gold working electrode and AgCl reference electrode at pH ~12.0, with a collection rate of 2.00 Hz using the "Gold, Carbo, Quad" waveform. A wash injection of only water was performed after 14 samples. Dionex Chromeleon 7 Chromatography Data System (Thermo Fisher Scientific) was used to process the chromatograms. Standards of glucose, galactose, fructose, sucrose and lactose were run. Selected samples were spiked with these sugars to confirm identity or absence of peaks.

Plasma and PBMC proteomics analysis

Samples were lysed (PBMC samples) or diluted (plasma samples) in SDS solubilization buffer (5% SDS, 50 mM TEAB, pH 7.5), heated at 95°C for 10 min and probe-sonicated before determining protein concentration using BCA (Thermo Scientific). The lysed samples were denatured and alkylated by adding TCEP (Tris(2-carboxyethyl) phosphine hydrochloride, Thermo Scientific) and CAA (2-chloroacetamide, Sigma) to a final concentration of 10 mM and 40 mM, respectively, and the mixture was incubated at 55°C for 15 min. Sequencing grade trypsin and Lys-C (Promega) was added (1:50 enzyme:protein ratio) and incubated overnight at 37°C after the proteins were trapped using S-Trap mini columns (Profiti). Tryptic peptides were eluted from the columns using (i) 50 mM TEAB (triethylammonium bicarbonate), (ii) 0.2% formic acid and (iii) 50% acetonitrile, 0.2% formic acid. The fractions were pooled, concentrated, and reconstituted in 200 mM HEPES, pH 8.5. Using a Pierce Quantitative Colorimetric Peptide Assay Kit (Thermo Scientific), equal peptide amounts of each sample were labelled with the TMTpro 16plex reagent set (Thermo Scientific) according to the manufacturer's instructions and considering a labelling strategy to minimize channel leakage. Individual samples were pooled and high-pH RP-HPLC was used to fractionate each pool into

Open Access Article. Published on 31 March 2026. Downloaded on 4/2/2026 12:19:51 AM.
This article is licensed under a Creative Commons Attribution 3.0 Unported Licence.

Food & Function Accepted Manuscript

View Article Online
DOI: 10.1039/D5FO04456A

Open Access Article. Published on 31 March 2026. Downloaded on 4/2/2026 12:19:51 AM.
This article is licensed under a Creative Commons Attribution 3.0 Unported Licence.

Food & Function Accepted Manuscript

fractions, then individually acquired by LC-MS/MS. Using a Dionex UltiMate 3000 RSLCnano system equipped with a Dionex UltiMate 3000 RS autosampler, an Acclaim PepMap RSLC analytical column (75 µm x 50 cm, nanoViper, C18, 2 µm, 100Å; Thermo Scientific) and an Acclaim PepMap 100 trap column (100 µm x 2 cm, nanoViper, C18, 5 µm, 100Å; Thermo Scientific), the tryptic peptides were separated by increasing concentrations of 80% acetonitrile (ACN) / 0.1% formic acid at a flow of 250 nl/min for 158 min and analyzed with an Orbitrap Fusion Tribrid (for PBMC samples) and an Orbitrap Eclipse Tribrid (for plasma samples) mass spectrometer (both ThermoFisher Scientific). In brief, the instruments were operated in data-dependent acquisition mode to automatically switch between full scan ms1 (in Orbitrap), ms2 (in ion trap) and ms3 (in Orbitrap) acquisition using Synchronous Precursor Selection.

All raw data files were analyzed with Sequest embedded in Proteome Discoverer (Thermo Scientific) to obtain quantitative ms3 reporter ion intensities, which were further analyzed using in-house generated R packages. Database searching was performed with the following parameters: carbamidomethylation at cysteine residues as well as TMTpro at peptide N-termini and lysine residues were selected as fixed modification, whilst oxidation of methionine and acetylation of protein N-termini were set as variable modifications. A false discovery rate (FDR) of 1% was allowed for both protein and peptide identification, and a human protein sequence database downloaded from Uniprot/SwissProt in June 2020 was underlying all searches. For proteomics data, analyses were performed using R (version 4.2.2). First, the dataset was filtered for high confidence and contaminant proteins, and proteins with missing values were removed. The data were normalized using reference channels by Internal Reference Standard (IRS) and Variance stabilizing normalization (vsn) methods. The protein intensity data were converted to log2 scale. To assess changes over time, a one-way ANOVA

View Article Online
DOI: 10.1039/D5FO04456A

was performed with FDR adjustment for multiple comparisons, and for significant results, a Tukey post-hoc test was performed for comparisons of each time point with 0-min. Proteins with adjusted-*p*-value < 0.05 were used for gene ontology (GO) analyses using ClueGO with CluePedia plugin (v 2.5.9) (39) within Cytoscape v.3.9.1 (40) to identify and visualize biological processes that were impacted after consumption of the HFHCM. Biological processes were considered significant with an adjusted-*p*-value < 0.01 after Bonferroni correction.

Statistical analyses

The power calculation was based on the primary outcome of postprandial plasma MPO. A total of 15 participants was originally calculated to be sufficient to determine statistically significant differences in MPO activity before and after a challenge meal at 95% power, with an α value of 0.05, based on values previously reported (41). However, COVID restrictions at the time of the study meant that we were only able to recruit and complete 12 subjects. Nevertheless, this was sufficient to see a change in the primary outcome both as MPO protein measured by ELISA, and in MPO products as measured by metabolomics. All statistical analyses were performed using the Statistical Package for Social Sciences (SPSS) version 28 (SPSS Inc., Chicago, IL, USA) and GraphPad Prism 9.0.1 (GraphPad Software, Boston, MA, USA). The Shapiro-Wilk test was used to assess data distribution. Where the majority of time-points were not normally distributed (TGs, insulin), data were log-transformed for statistical analysis. Differences over time for MPO, SOD1, glucose, insulin, and TGs were analyzed by repeated measures ANOVA, with time as the within-subjects factor, with Dunnet's multiple comparisons post hoc test, and adjusted *p*-values are reported. White blood cell counts were analyzed using a repeated measures ANOVA with time as the within-subjects factor. Tukey multiple comparisons post hoc tests were applied, and adjusted *p*-values reported. Magnitude

Open Access Article. Published on 31 March 2026. Downloaded on 4/2/2026 12:19:51 AM.
This article is licensed under a Creative Commons Attribution 3.0 Unported Licence.

Food & Function Accepted Manuscript

View Article Online
DOI: 10.1039/D3FO04456A

Open Access Article. Published on 31 March 2026. Downloaded on 4/2/2026 12:19:51 AM.
This article is licensed under a Creative Commons Attribution 3.0 Unported Licence.

Food & Function Accepted Manuscript

of change was calculated by deducting the fasting value (0 min) from the highest concentration for MPO, glucose, insulin, and TGs and lowest concentration for SOD1. Area under the curve (AUC) and incremental AUC (iAUC) were calculated for the postprandial period (0 to 360 min) for glucose, TG, MPO, and SOD1. The AUC, which is reflective of total blood concentration levels over time, was calculated using the trapezoidal rule by adding together measurements at adjacent time points, multiplying by the time between each measure, and dividing by 2. The iAUC represents only the area above baseline, showing the impact of the meal independent of fasting values. The iAUC was calculated using the trapezoidal rule by subtracting the 0-min value from all measurements to get a baseline-adjusted measurement, adding together measurements at adjacent time points, multiplying by the time between each measure, and dividing by 2. Where baseline-adjusted values were below zero, only the area above zero was calculated. The iAAC was calculated for SOD1 for the postprandial period (0 to 360 min) to indicate the decreased postprandial response, and was calculated using the same method as iAUC, but converting all negative values to positive and vice versa to get the area "above" the curve. Based on the mechanisms linking MPO and SOD1 with glucose and lipid levels, two-tailed Pearson correlations were used to determine whether there were associations between the oxidative stress markers (fasting (0 min), postprandial AUC/iAUC/iAAC, and magnitude of change) and glucose and triglyceride levels (fasting (0 min), postprandial iAUC, and magnitude of change).

View Article Online
DOI: 10.1039/D5FO04456A

Open Access Article. Published on 31 March 2026. Downloaded on 4/2/2026 12:19:51 AM.
This article is licensed under a Creative Commons Attribution 3.0 Unported Licence.

Food & Function Accepted Manuscript

Results

Participant characteristics and composition of the HFHCM

Participant characteristics, recruitment summary and study design are summarized in **Figure 1**. The HFHCM (90 kJ/kg body weight) was analyzed for macronutrient content (**Table 1**). The energy contribution was 16% from protein, 48% from carbohydrates (mostly mono- and di-saccharides) and 36% from fat (of which 82% was saturated fatty acids). The predominant amino acids were glutamic acid/glutamine and proline, and the most abundant fatty acids were lauric acid (C12:0) and palmitic acid (C16:0). There were no adverse effects, although subjects felt very full after consuming the meal, and one experienced mild nausea. Compliance was 100% as all subjects were observed to consume the meal.

Postprandial changes in glucose, insulin and triglycerides, and MPO

The study design facilitated measurement of any changes during a control period of 2 hours, followed by a postprandial period of 6 hours. This design was used to minimize intra-individual and day-to-day variation in volunteer responses. During the fasting control period of 120 min in 12 healthy young men, blood levels of glucose, insulin, triglycerides, and MPO remained stable. On subsequent consumption of a single HFHCM, postprandial glucose ($p = 0.005$) and insulin ($p < 0.0001$) concentrations peaked at 30 min, whereas mean circulating triglyceride levels were still increasing at 360 min ($p < 0.0001$) (**Figure 2)**. The relatively low glucose concentrations indicate good insulin sensitivity as expected in this cohort of young, healthy males. Serum MPO protein concentration, as assessed by ELISA, transiently increased over time ($p = 0.018$, $t_{max} = 180$ min) (**Figure 2**) but showed substantial inter-individual variability.

Postprandial changes in the plasma metabolome showed multiple patterns of change for amino acids, fatty acids and sugars

View Article Online
DOI: 10.1039/D5FO04456A

Open Access Article. Published on 31 March 2026. Downloaded on 4/2/2026 12:19:51 AM.
This article is licensed under a Creative Commons Attribution 3.0 Unported Licence.

Food & Function Accepted Manuscript

449 A total of 1,234 metabolites were putatively identified in the plasma samples and the number
450 of metabolites that changed at each experimental time point (defined as $p < 0.01$), with no
451 change in the control period, are shown in **Figure 2.** Various classes of metabolites showed a
452 time-dependent effect and details of all metabolites that changed during the experimental
453 period, grouped into compound class, are shown in **Supplementary Tables 1-7**. Potential
454 products of MPO action, namely L-methionine S-oxide, an oxidized metabolite of methionine
455 (42, 43), 3-(4-hydroxyphenyl)pyruvate, an oxidized metabolite of tyrosine (44), and L-
456 homocitrulline, an oxidized metabolite of lysine (45, 46), were increased after the HFHCM
457 (**Figure 2**).
458
459 Due to the high number of possible isomers and the nature of mass spectrometry, the
460 monosaccharides and disaccharides could not be unambiguously assigned from the
461 metabolomic analysis. We therefore assessed the sugars in plasma by (HPAEC-PAD) (**Figure**
462 **2)**. A similar response pattern was observed for glucose measured chromatographically by
463 HPAEC-PAD and by the automated hexokinase-based assay. Galactose was not detected
464 during fasting, then rapidly increased after the HFHCM (t_{max} = 150 min). Fructose was present
465 in low concentrations during fasting and increased after the HFHCM (t_{max} = 120 min). The
466 disaccharides, sucrose and lactose, despite a high concentration in the HFHCM, were not
467 detected in the plasma at any time point.
468
469 Plasma amino acids are shown in **Figure 3**. Despite glutamic acid/glutamine being the most
470 abundant amino acids measured in the HFHCM, they did not increase in plasma during the
471 postprandial period. Proline was high in the HFHCM, was highly abundant in plasma at fasting,
472 increased after consumption of the HFHCM, and remained elevated at 360 min. Valine,
473 leucine, phenylalanine, tyrosine, methionine, and isoleucine were also increased after

View Article Online
DOI: 10.1039/D5FO04456A

Open Access Article. Published on 31 March 2026. Downloaded on 4/2/2026 12:19:51 AM.
This article is licensed under a Creative Commons Attribution 3.0 Unported Licence.

Food & Function Accepted Manuscript

consumption of the HFHCM, and remained elevated at 360 min. Alanine and threonine were increased at 60 and 120 minutes, but had returned to baseline by 360 min. Cysteine and glycine were not measured by the metabolomics analysis. Additionally, two nitrogen-containing organic acids, creatine and phenacetylglycine, increased after the meal and remained elevated at 360 minutes (**Figure 3**).

Various free fatty acids in plasma were changed after the HFHCM, with the saturated fatty acids C8:0, C10:0 and C12:0 all increasing with time after the meal. In fact, C12:0 was one of the least abundant fatty acids in plasma during the control fasting phase, but at 360 min was one of the most abundant, owing to the high concentration in the meal. Many of the other fatty acids transiently decreased at 60 and 120 min followed by an increase back towards fasting levels (C16:0, C18:0, C18:1, and C18:2),or exceeding fasting levels (C14:0) at 360 min (**Figure 4**). Many less abundant fatty acids and putative oxo-fatty acids transiently decreased and most returned to baseline at 360 min, whereas hydroxy-fatty acids decreased, except for C18:2 derivatives (**Supplementary Table 2**). Several dicarboxylic acids, products of ω-oxidation, showed a substantial increase (**Supplementary Table 2**).

Postprandial changes in other metabolites

Acetylcarnitine, and most other acylcarnitines that showed a change, decreased after the HFHCM, whereas propionyl carnitine was one of the very few carnitine derivatives that increased. The full profile of carnitines that changed are shown in **Supplementary Table 3**. Most phosphatidylcholines that changed decreased at 60 and 120 min, and returned to baseline at 360 min. Of the phosphatidylethanolamines, phosphatidylinositols and lysophospholipids that showed a postprandial change, most showed an increase and were still elevated from the baseline at 360 min (**Supplementary Table 4**). Plasma bilirubin showed an immediate

View Article Online
DOI: 10.1039/D3FO04456A

Open Access Article. Published on 31 March 2026. Downloaded on 4/2/2026 12:19:51 AM.
This article is licensed under a Creative Commons Attribution 3.0 Unported Licence.

Food & Function Accepted Manuscript

decrease after the HFHCM, whereas bilirubin metabolites increased and were still high at 360 min (**Figure 4**). Cholate derivatives that changed showed a rapid increase and then a slow decrease (**Figure 4**), whereas cholesterol sulfate showed an increase at 360 min (**Supplementary Table 2**). Some di- and tripeptides changed after the HFHCM, with the most abundant dipeptide, isoleucine-proline, decreasing at 360 min (**Supplementary Table 5**). Putatively identified hydroxy-isocaproic acid is an obligate microbial metabolite and increased at 6 hour ($p<0.01$) (**Figure 4)**. Other metabolites including pyruvate, a product of glycolysis which transiently increased, are shown in **Supplementary Table 6**. There were a substantial number of unknown metabolites which could not be identified from the databases. Their exact masses are shown in **Supplementary Table 7**. There were also many metabolites which were tentatively identified but could not be found in the human metabolite database. Since the database is mostly constructed from data derived from fasting samples, it is possible that some metabolites could have been correctly identified but only present in postprandial blood samples. All of the unknown metabolite data provides a resource for future discoveries (**Supplementary Table 7).** Since the changes are complex and time-dependent, we constructed a graphical representation of the metabolite changes, which we term a postcibalmetabolome, allowing identification of patterns of changes in groups of metabolites (**Figure 5)**.

Postprandial changes in the plasma proteome were related to oxidative stress

There were 1,568 proteins identified in the plasma samples, of which 515 proteins had no missing values across all participants and time points. During the fasting control phase, there were very few significant changes in plasma proteins. After the HFHCM, some changes in the abundance of certain proteins became apparent at 180 min, with increasing numbers at 240 and 300 min, before most proteins returned back to baseline at 360 min (**Figure 6**). The 12 most abundant proteins in plasma (albumin, α-2-macroglobulin, apolipoprotein B, complement C3,

View Article Online
DOI: 10.1039/D5FO04456A

transferrin, serpin family A member 1, apolipoprotein A1, haptoglobin, complement C4A, fibrinogen α-chain, immunoglobulin heavy constant α-1 and apolipoprotein A2) did not change significantly at any time point (**Figure 6**), but otherwise, changes were observed in 219 proteins (defined as ANOVA adjusted *p*-value < 0.05) present at a wide range of initial concentrations. Ontology analysis of the proteins showed that they could be grouped into 17 biological processes (**Table 2**). The largest group of proteins were clustered into the pathway termed "cellular oxidant detoxification", which is shown as a network with all first-degree proteins and GO classes that were changed after the meal (**Figure 6**). Almost all of the proteins included in this network were decreased at 240 and 300 min. Several well-known plasma antioxidants decreased after consumption of the meal, including catalase (CAT), thioredoxin (TXN), glutathione peroxidase 1 (GPX1), (**Figure 7**) and peroxiredoxins (PRDX)-1, PRDX-2, PRDX-3, and PRDX-6 (**Supplementary Table 8**). One of the notable proteins was Cu/Zn-superoxide dismutase (SOD)-1, which transiently decreased at both 240 ($\log_2$ fold change = -0.11, $p < 0.0001$) and 300 ($\log_2$ fold change = -0.10, $p < 0.0001$) minute time points (**Figure 7**). To confirm this, we assessed SOD1 protein by quantitative ELISA and the results were in excellent agreement with the proteomic analysis, but additionally showed decreased concentrations at 30, 90 and 150 min (time points not measured by proteomic analysis) compared with fasting ($p < 0.05$) (**Figure 7**). From the proteomics data, we also observed that Mn-SOD2 decreased at 240 and 300 min, but extracellular SOD3, which was at lower levels in plasma, did not change at any time point (**Figure 7**).

Plasma SOD1 levels were associated with fasting and postprandial plasma glucose

Substantial inter-individual differences allowed correlations between biomarkers from individual volunteers to be assessed. There were no associations between fasting or postprandial MPO or SOD1 protein with circulating TG levels. Fasting and postprandial MPO

Open Access Article. Published on 31 March 2026. Downloaded on 4/2/2026 12:19:51 AM.
This article is licensed under a Creative Commons Attribution 3.0 Unported Licence.

Food & Function Accepted Manuscript

View Article Online
DOI: 10.1039/D5FO04456A

Open Access Article. Published on 31 March 2026. Downloaded on 4/2/2026 12:19:51 AM.
This article is licensed under a Creative Commons Attribution 3.0 Unported Licence.

Food & Function Accepted Manuscript

protein also showed no association with fasting or postprandial glucose concentrations (**Supplementary Table 9**). However, fasting glucose was negatively associated with SOD1 protein fasting levels (r = -0.630, p = 0.028), iAAC (r = -0.600, p = 0.039), and magnitude of change (r = -0.584, p = 0.046) (**Figure 7**). Glucose postprandial AUC also showed strong negative associations with SOD1 protein fasting concentration (r = -0.774, p = 0.003), iAAC (r = -0.723, p = 0.008) and magnitude of change (r = -0.767, p = 0.004) (**Figure 7**). Glucose magnitude of change (peak concentration minus time zero concentration) showed no associations with any measure of SOD1 protein. Details of the SOD1 associations are shown in **Supplementary Table 10**.

White blood cell counts and the PBMC proteome were minimally affected by the HFHCM

There were no changes in total white blood cells, monocytes, or neutrophil cell counts. Lymphocyte and eosinophil cell counts slightly decreased over time (p = 0.026, and p = 0.034, respectively) during the postprandial period (**Supplementary Table 11**). Basophils were not detected at any time point.

We also assessed changes in the PBMCs by proteomic analysis of the intracellular proteins at 0, 180 and 360 min. There were 6,698 proteins detected in the analysis, of which 4,105 proteins had no missing values across all participants and time points. However, the PBMC proteome was quite robust and hardly affected by the HFHCM, since the ANOVA analysis only identified 38 of the 4,105 proteins that were changed in response to the meal. After the meal, changes were observed in levels of 17 proteins (7 increased), and 35 proteins (11 increased) at 180 min and 360 min, respectively. Fourteen of the proteins that changed at 180 min remained changed at 360 min (**Supplementary Table 12**). Ontology analyses could not reveal any biological processes owing to the small number of proteins that were changed in response to the HFHCM. However, a handful of proteins were aligned with the biological processes that

View Article Online
DOI: 10.1039/D5FO04456A

were enriched in the plasma proteome during the postprandial period. While 'Cellular Oxidant Detoxification' proteins were decreased in plasma, several proteins related to oxidative stress and inflammation (CYB5B, DHRS4, NQO2, HMGB1, and CFDP1) were all increased in PBMCs ($p < 0.05$). Similarly, proteins associated with 'generation of precursor metabolites and energy' were decreased in the plasma proteome at 240 and 300 min, yet RWDD1 (cellular response to lipid), IDI1 (cholesterol synthesis), SLC2A3 (glucose transport) and ATP5EP2 (energy metabolism) were all increased in the PBMCs following consumption of the HFHCM ($p < 0.05$) (**Supplementary Table 12**).

Open Access Article. Published on 31 March 2026. Downloaded on 4/2/2026 12:19:51 AM.
This article is licensed under a Creative Commons Attribution 3.0 Unported Licence.

Food & Function Accepted Manuscript

View Article Online
DOI: 10.1039/D5FO04456A

Open Access Article. Published on 31 March 2026. Downloaded on 4/2/2026 12:19:51 AM.
This article is licensed under a Creative Commons Attribution 3.0 Unported Licence.

Food & Function Accepted Manuscript

Discussion

This postprandial study is the first to use multi-omics in combination with several conventional metabolic markers to examine in detail the acute response to a HFHCM, which we originally considered would be an extreme example of an ultra-processed food with a well-defined nutrient composition. Using multiple time-points across both fasting and post-meal periods (from -2 to 6 hours) in healthy men, we identified 1,568 plasma proteins, 4,105 peripheral blood mononuclear cell proteins and 1,234 plasma metabolites. After the HFHCM, processes at multiple levels contributed to an increase in oxidative stress markers with lowered defenses. Proteins in the plasma are predominantly secreted by solid tissues, which include the classical plasma proteins from the liver and intestine, as well as “long distance” receptor ligands, including peptide and protein hormones such as insulin and glucagon-like peptide-1 (47). After the HFHCM, a substantial number of proteins (~5 % of total) normally present in the plasma, decreased at 240 and 300 min, returning to baseline levels by 360 min. The predominant group of proteins were classified as “cellular oxidant detoxification” and included Cu/Zn-SOD1 and Mn-SOD2. While no studies have previously measured plasma SOD1 or SOD2 protein levels as a biomarker of postprandial oxidative stress, patients with type 2 diabetes have lower postprandial plasma SOD activity (SOD isoform not specified) (48) and lower fasting SOD activity (49-51) compared with healthy controls. Lowered SOD1 levels have been linked with increased oxidative stress and increased risk of vascular diseases, while elevated SOD1 promotes vascular protection (52). Inter-individual differences allowed us to determine that the magnitude of the decrease in SOD1 protein was negatively associated with both fasting and total glucose, indicating that higher fasting glucose is associated with loss of antioxidant defense capacity. This is further supported in a diabetic rat model, where direct administration of SOD1 protein decreased fasting blood glucose (53). We propose that the oxidative defense

View Article Online
DOI: 10.1039/D5FO04456A

Open Access Article. Published on 31 March 2026. Downloaded on 4/2/2026 12:19:51 AM.
This article is licensed under a Creative Commons Attribution 3.0 Unported Licence.

Food & Function Accepted Manuscript

proteins, especially SOD1, could be used as postprandial biomarkers to assess the protective effects of nutrients, micronutrients and phytochemicals when consumed with a meal.

Alongside the decreased antioxidant defense proteins, there were increases in stress-related enzymes and products, which could potentially be used as biomarkers of protection against postprandial stress. The increase in MPO and its products is a good example. Increased levels of certain plasma lipids, such as after a meal, can stimulate the release of MPO from monocytes (41, 54), which is readily absorbed by the vascular endothelium (41, 55) and impairs endothelial function by interfering with nitric oxide signaling (56). It is most likely that the high-fat component of the HFHCM led to the postprandial increase in MPO, since a decrease in postprandial MPO levels has been observed following consumption of glucose alone (29). High-fat feeding also increases production of MPO in the gut of rodents (57, 58). Other potential biomarkers are the products of oxidative stress, such as hydroxy-fatty acids from lipid peroxidation, dicarboxylic acids from ω-oxidation, creatine, present in the milk component of the HFHCM but also a marker of mitochondrial dysfunction (59), and phenacetylglycine, a product of mitochondrial dysfunction (60).

We hypothesize that when food, especially fat, reaches the microbiota, the colon tissue may become metabolically stressed. The appearance of microbiota-specific metabolites in plasma, such as bilirubin metabolites (64), short chain fatty acids, and hydroxyisocaproic acid (65), were seen at a similar time to the lowering of antioxidant and other proteins. One manifestation of the increased nutrient content introduced to the colonic microbiota could be for the colonocytes to temporarily secrete lower amounts of protective antioxidant enzymes into the blood, since the proteins would be required for maintaining intracellular function and protection from oxidative stress due to accelerated glycolysis and fatty acid β-oxidation.

Consumption of the HFHCM increased plasma levels of valine, leucine, phenylalanine, tyrosine, isoleucine, proline and methionine, which all remained elevated at 360 min. These

View Article Online
DOI: 10.1039/D5FO04456A

Open Access Article. Published on 31 March 2026. Downloaded on 4/2/2026 12:19:51 AM.
This article is licensed under a Creative Commons Attribution 3.0 Unported Licence.

Food & Function Accepted Manuscript

amino acids are also elevated in the fasting blood of a high diabetes-risk phenotype observed following a meta-analysis including 8,000 individuals (61). It is noteworthy that this profile of plasma amino acids was not directly comparable with amino acid levels measured in the meal. Postprandial free-carnitine remained constant, but serum acetylcarnitine, synthesized in mitochondria, was decreased after the HFHCM, consistent with observations that acetylcarnitine increases during exercise or starvation (62). Many phospholipids also changed after the HFHCM, with some remaining elevated at 360 min, although the absolute identification of isomers is tentative.

In our recent systematic review (63), we only found 2 papers that examined the postprandial PBMC proteome, with major discrepancies between them. Circulating PBMCs exist in an environment that fluctuates in nutrients, proteins, hormones, products of oxidative stress and many other factors after a meal, and so some modulation of function might be expected, especially since *ex vivo* experiments have shown changes in monocytes exposed, for example, to certain fatty acids (41). Our review reported consistent postprandial transcriptomic changes in PBMCs, where four major processes are affected by a high fat meal; inflammation/oxidative stress, GTP metabolism, apoptosis, and lipid localization/transport (63). However, analysis of the proteome of PBMCs showed that despite the high number of proteins that were identified, remarkably low numbers of proteins changed after the meal. The changes were too few to be formally categorized into pathways, but notable gene functions were similar to changes in the transcriptome of PBMCs, and were related to oxidative stress: CYB5B, involved in nitric oxide biosynthesis, the redox active DHRS4, and the antioxidant enzyme NQO2; phosphorylation, including IMPAD1, PPP1CA, GIGYF2 and SHOC2; and energy metabolism, including the glucose transporter SLC2A3 (GLUT3), an ATP synthase (ATP5EP2) and RWDD1 involved in cellular responses to lipids. The full list is shown in **Supplementary Table 2**.

View Article Online
DOI: 10.1039/D5FO04456A

Open Access Article. Published on 31 March 2026. Downloaded on 4/2/2026 12:19:51 AM.
This article is licensed under a Creative Commons Attribution 3.0 Unported Licence.

Food & Function Accepted Manuscript

Strengths of the study are: a) incorporating both control and experimental periods, which lowers the effects of intra-individual variation, b) the use of a well-characterized HFHCM, and c) recruitment of healthy young male participants with good metabolic flexibility. The main limitations are that the outcomes cannot be generalized to different population groups such as females, older people, or metabolically dysfunctional individuals, and future studies are needed to facilitate this. Although the sample size (n=12) is small, it provided enough power to detect a change in the main outcome, and the cost of proteomic and metabolomic analyses at multiple time points per person limited the number of volunteers we could use. Twelve people completed instead of 15 owing to COVID lockdowns at the time, but this still proved sufficient to observe a change in the primary outcome. Although we found statistically-significant associations between some markers, the number of data points is low for this type of correlation. Further, this acute postprandial study does not elucidate the effects of habitual consumption of HFHCM, but instead provides the biomarkers necessary to estimate the effects of multiple HFHCM on chronic metabolic dysfunction when using a stress meal.

Poor diets are typified by low micronutrient, dietary fiber and phytochemical contents, together with high saturated fat, sodium and sugar content. The results of this study demonstrate that a single HFHCM induces an acute, transient metabolic and oxidative stress response which is apparent at protein and metabolite levels. In healthy volunteers, the ability to rapidly adapt to postprandial nutrient overload and oxidative stress restores fasting homeostasis and prevents undesirable side-effects. However, repeated consumption of such meals could lead to over-burden of the systemic redox-system, and ultimately result in metabolic dysfunction.

The main limitation of the study is that the cohort were only healthy young men, and future studies would need to examine a wider cohort. On the other hand, this report is by far the most comprehensive multi-omics analysis of the postprandial response to a HFHCM, and uncovers

View Article Online
DOI: 10.1039/D5FO04456A

multiple new responses of interlinked metabolic changes and adaptation that may lead to chronic metabolic dysfunction with regular consumption of ultra-processed foods. We previously introduced the concept of the postcibalome (63), which are all of the multi-level complex changes that occur after a meal. We also here introduce the postcibalmetabolome (**Figure 5**), which provides a visual way to assess all metabolite changes in a study. We identify new tools for assessing the acute effects of nutrients and phytochemicals to protect metabolic flexibility and reduce the stress induced by high saturated fat-high refined carbohydrate food such as ultra-processed foods.

Open Access Article. Published on 31 March 2026. Downloaded on 4/2/2026 12:19:51 AM.
This article is licensed under a Creative Commons Attribution 3.0 Unported Licence.

Food & Function Accepted Manuscript

View Article Online
DOI: 10.1039/D5FO04456A

Open Access Article. Published on 31 March 2026. Downloaded on 4/2/2026 12:19:51 AM.
This article is licensed under a Creative Commons Attribution 3.0 Unported Licence.

Food & Function Accepted Manuscript

CRediT authorship statement

Aimee L Dordevic: Conceptualization, Methodology, Formal analysis, Visualization; Writing original draft, Writing – review and editing, Supervision; Margaret Murray: Project administration, Investigation, Writing original draft, Writing – review and editing; Michael J Houghton: Methodology; Investigation, Formal analysis; Writing – review and editing; Nina M Trinquet: Investigation, Writing – review and editing; Nicole J Kellow: Investigation, Writing – review and editing; Ralf B Schittenhelm: Investigation, Writing – review and editing; Christopher K Barlow: Investigation, Writing – review and editing; Kaitlin Day: Formal analysis, Writing – review and editing; Louise Bennett: Conceptualization, Funding acquisition; Writing – review and editing; Beau-Luke Colton: Methodology, Investigation, Writing – review and editing; Gary Williamson: Conceptualization, Methodology, Formal analysis, Visualization; Funding acquisition; Writing original draft, Writing – review and editing, Supervision

Declarations of interests

ALD has received research funding from the Australian Government Department of Industry, Science, Energy and Resources, Innovation Connections Grant, with Melrose Laboratories Pty Ltd as partner. ALD and MJH have received research funding from ViPlus Nutritional Australia Pty Ltd. MJH has received research funding from Northern Nut Growers Association Inc., USA. GW is on the Scientific Advisory Board for Nutrilite, USA, and receives funding from Nutrilite USA, The Product Makers (TPM) Australia and from an Australia Research Council Linkage Project (LP210200616) with Heinz as partner. None of these companies or projects were involved in the research reported here. The other authors report no conflict of interest.

View Article Online
DOI: 10.1039/D5FO04456A

Open Access Article. Published on 31 March 2026. Downloaded on 4/2/2026 12:19:51 AM.
This article is licensed under a Creative Commons Attribution 3.0 Unported Licence.

Food & Function Accepted Manuscript

Acknowledgements

The authors would like to acknowledge Natalie McPhee for plasma glucose and triglyceride analysis. This study used BPA-enabled (Bioplatforms Australia) / NCRIS-enabled (National Collaborative Research Infrastructure Strategy) infrastructure located at the Monash Proteomics and Metabolomics Platform. We thank Prof Andrew Sinclair and Prof Aedin Cassidy for critical reading of the manuscript.

Data availability

The metabolomics data have been submitted to the Metabolights platform (https://www.ebi.ac.uk/metabolights/) with the dataset identifier MTBLS10972. *The data will be made available following publication.*

The mass spectrometry proteomics data have been deposited to the ProteomeXchange Consortium via the PRIDE partner repository (https://www.ebi.ac.uk/pride/) with the dataset identifier PXD055358. *Before publication, the data are only available to reviewers: Username: reviewer_pxd055358@ebi.ac.uk; Password: BMzRoQsEgAg4.* The data will be made publicly available on publication of this work.

View Article Online
DOI: 10.1039/D5FO04456A

Table 1. Macronutrient analysis of the high fat/high carbohydrate challenge meal

Component	g per serving[1]	% of total mass
Carbohydrate	193.2	37.4
Protein	62.0	12.0
Fat	61.5	11.9
Saturated fatty acids	*50.5*	*9.77*
Monounsaturated fatty acids	*10.1*	*1.95*
Polyunsaturated fatty acids	*1.03*	*0.20*
Trans fatty acids	*0.31*	*0.06*
Moisture	187.0	36.2
Ash	12.9	2.5

Amino acids	Mole %	Fatty acids	Fat %
Histidine	2.4	C4:0 - Butyric acid	0.5
Serine	6.7	C6:0 - Caproic acid	0.8
Arginine	2.4	C8:0 - Octanoate	4.5
Glycine	3.3	C10:0 - Decanoate	4.6
Aspartic acid	7.4	C12:0 - Lauric acid	30.8
Glutamic acid	19.6	C14:0 - Myristic acid	15.7
Threonine	4.7	C16:0 - Palmitic acid	18.2
Alanine	4.9	C18:0 - Stearic acid	7.0
Proline	11.2	C16:1 - Palmitoleic acid (n-7)	0.9
Lysine	7.2	C18:1 - Oleic acid (n-9)	15.5
Tyrosine	2.2	C18:2 - Linoleic acid (n-6)	1.7
Methionine	2.0		
Valine	7.2	**Sugars**	**Carbohydrate %**
Isoleucine	5.4	Sucrose	19.5
Leucine	9.6	Lactose	70.1
Phenylalanine	3.8	Maltose	0.8
Histidine	2.4		

[1] Based on a 70 kg person. Total fat, protein, moisture and ash contents were established by proximate analysis, with total carbohydrate content obtained by subtraction. Amino acids, fatty acids, and sugars were analyzed separately as described in the methods section. Previously, challenge meals that have been used to induce postprandial oxidative stress include commercially available fast foods (20), nutritional supplements (19), and various combinations of high fat or high refined carbohydrate foods (15, 16, 18, 66, 67), but these are difficult to give on a per body weight basis. The response of postprandial oxidative stress markers can depend on the exact meal and composition, making comparison across studies difficult (68). Furthermore, some studies indicate that a HFHCM was given, but fail to provide any details about the ingredients or nutrient composition (17, 69). The meal developed here can be easily used by other labs, and is able to be administered on a per body weight basis.

Open Access Article. Published on 31 March 2026. Downloaded on 4/2/2026 12:19:51 AM.
This article is licensed under a Creative Commons Attribution 3.0 Unported Licence.

Food & Function Accepted Manuscript

View Article Online
DOI: 10.1039/D5FO04456A

741 **Table 2. Biological processes that were affected after the HFHCM.**

GO ID	Biological process name	% Proteins per group
GO:0098869	cellular oxidant detoxification	17.25
GO:0030168	platelet activation	14.08
GO:0030036	actin cytoskeleton organization	11.62
GO:0006091	generation of precursor metabolites and energy	10.56
GO:0031589	cell-substrate adhesion	6.34
GO:0006749	glutathione metabolic process	5.63
GO:0044183	protein folding chaperone	4.23
GO:0010634	positive regulation of epithelial cell migration	3.52
GO:0007599	hemostasis	3.52
GO:0097581	lamellipodium organization	3.17
GO:0097193	intrinsic apoptotic signaling pathway	3.17
GO:0005200	structural constituent of cytoskeleton	3.17
GO:0010810	regulation of cell-substrate adhesion	2.82
GO:0010631	epithelial cell migration	2.11
GO:0007596	blood coagulation	2.11
GO:0001667	ameboidal-type cell migration	2.11
GO:0034975	protein folding in endoplasmic reticulum	1.06

742 A one-way ANOVA was performed with FDR adjustment for multiple comparisons. Gene
743 ontology (GO) analyses were performed on proteins with adjusted-*p*-value < 0.05 using
744 ClueGO with CluePedia plugin (v 2.5.9) (39) in Cytoscape v.3.9.1 (40). Biological processes
745 were considered significant with an adjusted-*p*-value < 0.01 after Bonferroni correction.
746 Biological processes with < 1% proteins per group are not listed.

Open Access Article. Published on 31 March 2026. Downloaded on 4/2/2026 12:19:51 AM.
This article is licensed under a Creative Commons Attribution 3.0 Unported Licence.

Food & Function Accepted Manuscript

View Article Online
DOI: 10.1039/D5FO04456A

Open Access Article. Published on 31 March 2026. Downloaded on 4/2/2026 12:19:51 AM.
This article is licensed under a Creative Commons Attribution 3.0 Unported Licence.

Food & Function Accepted Manuscript

Figure legends

Figure 1. Key aspects of the study design. (A) Participant recruitment flow diagram, (B) participant characteristics and (C) simplified study design summary.

Figure 2. Postprandial changes in metabolic markers, myeloperoxidase and metabolites, and sugar analysis after a high-fat/high-carbohydrate meal.
Mean values (n = 12) for metabolic markers: plasma glucose (A), serum insulin (B), serum triglyceride (C), for MPO and metabolites: serum myeloperoxidase (MPO) (D), tentatively identified metabolites of MPO, L-homocitrulline (open black square); 3-(4-hydroxyphenyl)pyruvate (grey circle), and L-methionine S-oxide (black triangle) concentrations after a HFHCM. Panel (F) shows the total number (n) of changed metabolites that were identified from metabolomics analysis. Sugar analysis: HPAE-PAD chromatogram showing addition of internal standards (1 mg/L each) to enable positive peak identification: Unspiked (black line), fructose-spiked (purple line), and sucrose-spiked (blue line) (G), unspiked (black line) and lactose-spiked (orange line) (H). The relative peak areas after consumption of the HFHCM obtained using HPAE-PAD are shown for glucose (I), and sucrose (J). Plasma concentrations derived from HPAE-PAD relative peak areas are shown for galactose (K), and fructose (L). Control and experimental periods are indicated, allowing each participant to act as their own control. Values are mean ± standard error of the mean. Repeated measures ANOVA, and Dunnett, or Tukey (metabolomics) post-hoc analysis *p <0.05 **p < 0.01, ***p < 0.001, #p<0.05 main effect of time only.

Figure 3. Changes in amino acids after consumption of HFHCM.

View Article Online
DOI: 10.1039/D5FO04456A

Mean values (n = 12) for plasma glutamine and proline (A), histidine and valine (B), leucine, alanine, threonine and glutamate (C), lysine, phenylalanine, arginine and tyrosine (D), methionine, asparagine and isoleucine (E), tryptophan, serine and aspartate (F), creatine (G), and phenacetylglycine (H) concentrations before (control) and after (experimental) a HFHCM. Repeated measures ANOVA, and Tukey post-hoc analysis *p <0.05 **p < 0.01, ***p < 0.001.

Figure 4. Changes in fatty acids, microbiome metabolites, cholate derivatives and bilirubin/metabolites, after consumption of HFHCM.

Mean values (n = 12) for plasma C16:0, C18:1 and C18:2 (A), C8:0 and C12:0 (B), C10:0, C14:0 and C18:0 (C), C16:1 and C18:3 (D), C:20 and C21:0 (E), cholate derivatives, chenodeoxyglycholate (open black square), glycodeoxycholate (open grey circle), glycholate (grey inverted triangle), taurodeoxycholate (black triangle) (F), bilirubin (G), microbial derivatives of bilirubin, I-urobilinogen (black triangle), L-urobilin (open black square) (H), microbial derivatives of bilirubin, D-urobilinogen (open black square), I-urobilin (black triangle) (I), before (control) and after (experimental) a HFHCM. Repeated measures ANOVA, and Tukey post-hoc analysis *p <0.05 **p < 0.01, ***p < 0.001.

Figure 5: Postcibalmetabolome to visualize changes after a HFHCM.

Each metabolite within a group that changed after the HFHCM (p<0.01) is represented by a thin bar. The $\log_{10}$-fold change at the indicated times was calculated based on the peak area at the indicated time point divided by the mean value of the 3 relevant control time points. MPO, myeloperoxidase; sat, saturated; PC, phosphatidylcholine; PE, phosphatidyethanolamine; PI, phosphatidylinositol; Mw, molecular weight; Me, methylated.

Open Access Article. Published on 31 March 2026. Downloaded on 4/2/2026 12:19:51 AM.
This article is licensed under a Creative Commons Attribution 3.0 Unported Licence.

Food & Function Accepted Manuscript

View Article Online
DOI: 10.1039/D5FO04456A

Figure 6: Plasma proteomics and network analysis of plasma proteins that changed after the HFHCM: Cellular Oxidant Detoxification

Total proteins changing at each time point (A), -120 min (B), -60 min (C), 60 min (D), 120 min (E), 180 min (F), 240 min (G), 300 min (H), 360 min (I). Relative abundance of the twelve most abundant proteins in plasma showing no significant changes in the control nor experimental period (J). Panel (I) shows the biological process that was associated with the most changed proteins, 'Cellular Oxidant Detoxification' (grey) is visualized as a network containing links with all first-degree GO classes and plasma proteins that were changed after the HFHCM. using ClueGO with CluePedia plugin (v 2.5.9) (39) in Cytoscape v.3.9.1 (40). Proteins in the network are shown in the top four rows using their accepted gene names, and all were decreased at 240 and 300 min after the meal. The size of the GO class nodes depicts the percentage of associated proteins from that process. ALB, albumin; A2M, α-2-macroglobulin; APOB, apolipoprotein B; C3, complement C3; TF, transferrin; SERPINA1, serpin family A member 1; APOA1, apolipoprotein A1; HP, haptoglobin; C4A, complement C4A; FGA, fibrinogen α-chain; GHA1, immunoglobulin heavy constant α-1; APOA2, apolipoprotein A2.

Figure 7. Changes in plasma 'Cellular Oxidant Detoxification' proteins after the HFHCM, and correlations with plasma glucose.

Superoxide dismutase (SOD)-1, SOD2, and SOD3 (A), SOD1 protein levels measured by ELISA (B), catalase (CAT), thioredoxin (TXN), and glutathione peroxidase 1 (GPX1) (C). Repeated measures ANOVA, and Tukey or Dunnett's (SOD1 ELISA) post-hoc analysis *p <0.05 **p < 0.01, ***p < 0.001. Significant associations from Pearson two-tailed correlation analyses. Fasting glucose levels were negatively associated with SOD1 (A) fasting levels (r = -0.630, p = 0.028), (B) postprandial incremental area above the curve (iAAC, r = -0.600, p =

Open Access Article. Published on 31 March 2026. Downloaded on 4/2/2026 12:19:51 AM.
This article is licensed under a Creative Commons Attribution 3.0 Unported Licence.

Food & Function Accepted Manuscript

View Article Online
DOI: 10.1039/D5FO04456A

0.039), and (C) magnitude of change (r = -0.584, p = 0.046). Glucose postprandial area under the curve (AUC) was negatively associated with SOD1 (D) fasting levels (r = -0.774, p = 0.003), (B) postprandial iAAC (r = -0.723, p = 0.008), and (C) magnitude of change (r = -0.767, p = 0.004).

Open Access Article. Published on 31 March 2026. Downloaded on 4/2/2026 12:19:51 AM.
This article is licensed under a Creative Commons Attribution 3.0 Unported Licence.

Food & Function Accepted Manuscript

View Article Online
DOI: 10.1039/D5FO04456A

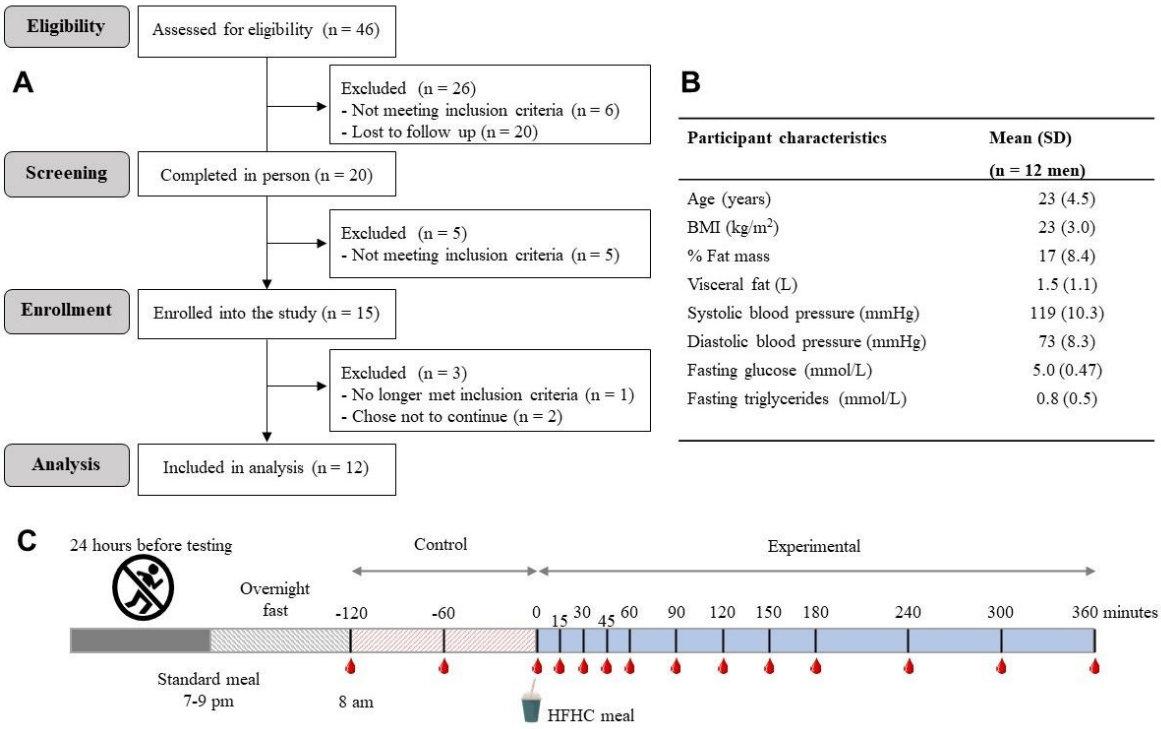

Participant characteristics	Mean (SD) (n = 12 men)
Age (years)	23 (4.5)
BMI (kg/m^2)	23 (3.0)
% Fat mass	17 (8.4)
Visceral fat (L)	1.5 (1.1)
Systolic blood pressure (mmHg)	119 (10.3)
Diastolic blood pressure (mmHg)	73 (8.3)
Fasting glucose (mmol/L)	5.0 (0.47)
Fasting triglycerides (mmol/L)	0.8 (0.5)

Figure 1.

Open Access Article. Published on 31 March 2026. Downloaded on 4/2/2026 12:19:51 AM.
This article is licensed under a Creative Commons Attribution 3.0 Unported Licence.

Food & Function Accepted Manuscript

View Article Online
DOI: 10.1039/D5FO04456A

Open Access Article. Published on 31 March 2026. Downloaded on 4/2/2026 12:19:51 AM.
This article is licensed under a Creative Commons Attribution 3.0 Unported Licence.

Food & Function Accepted Manuscript

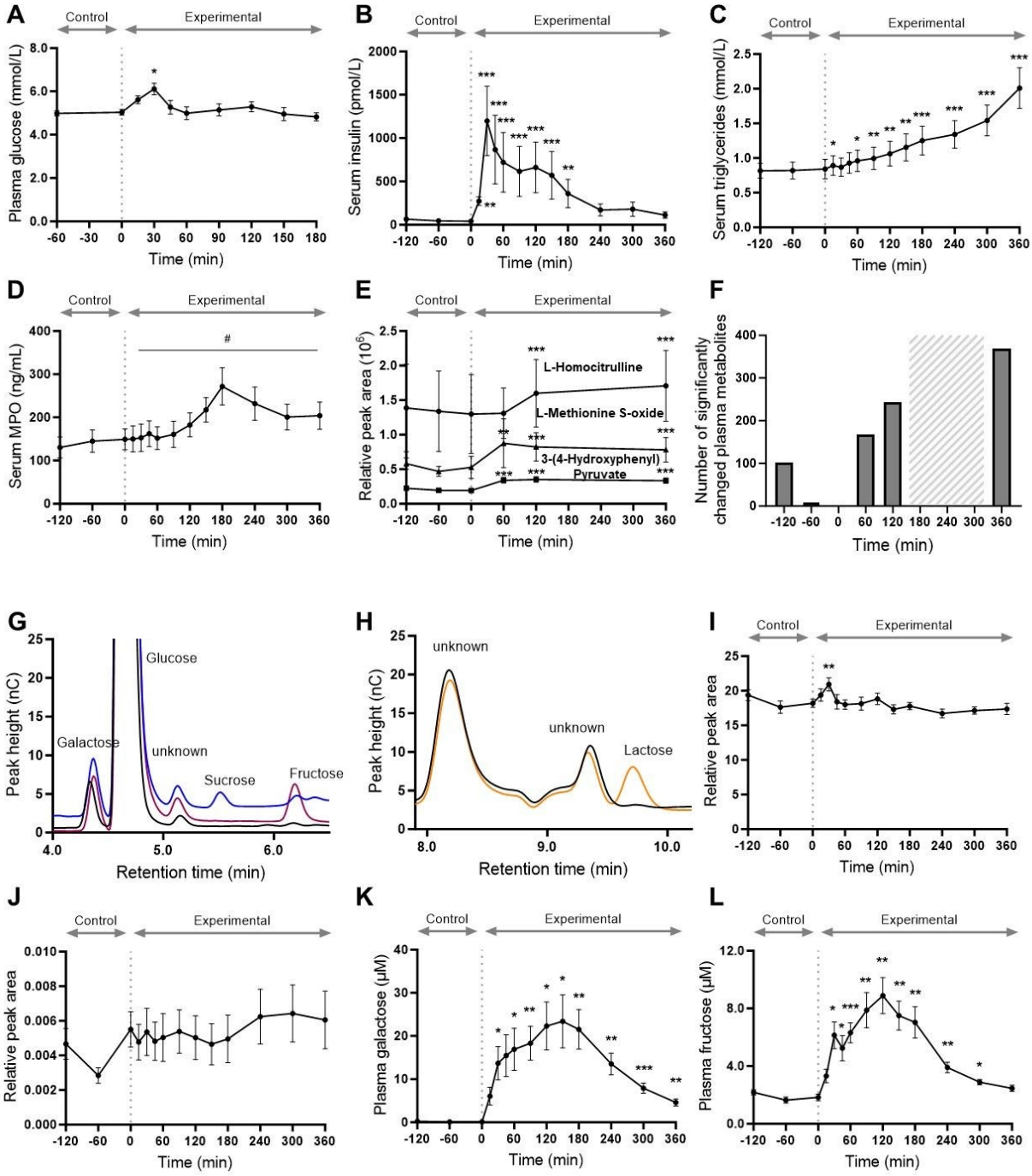

Figure 2.

View Article Online
DOI: 10.1039/D5FO04456A

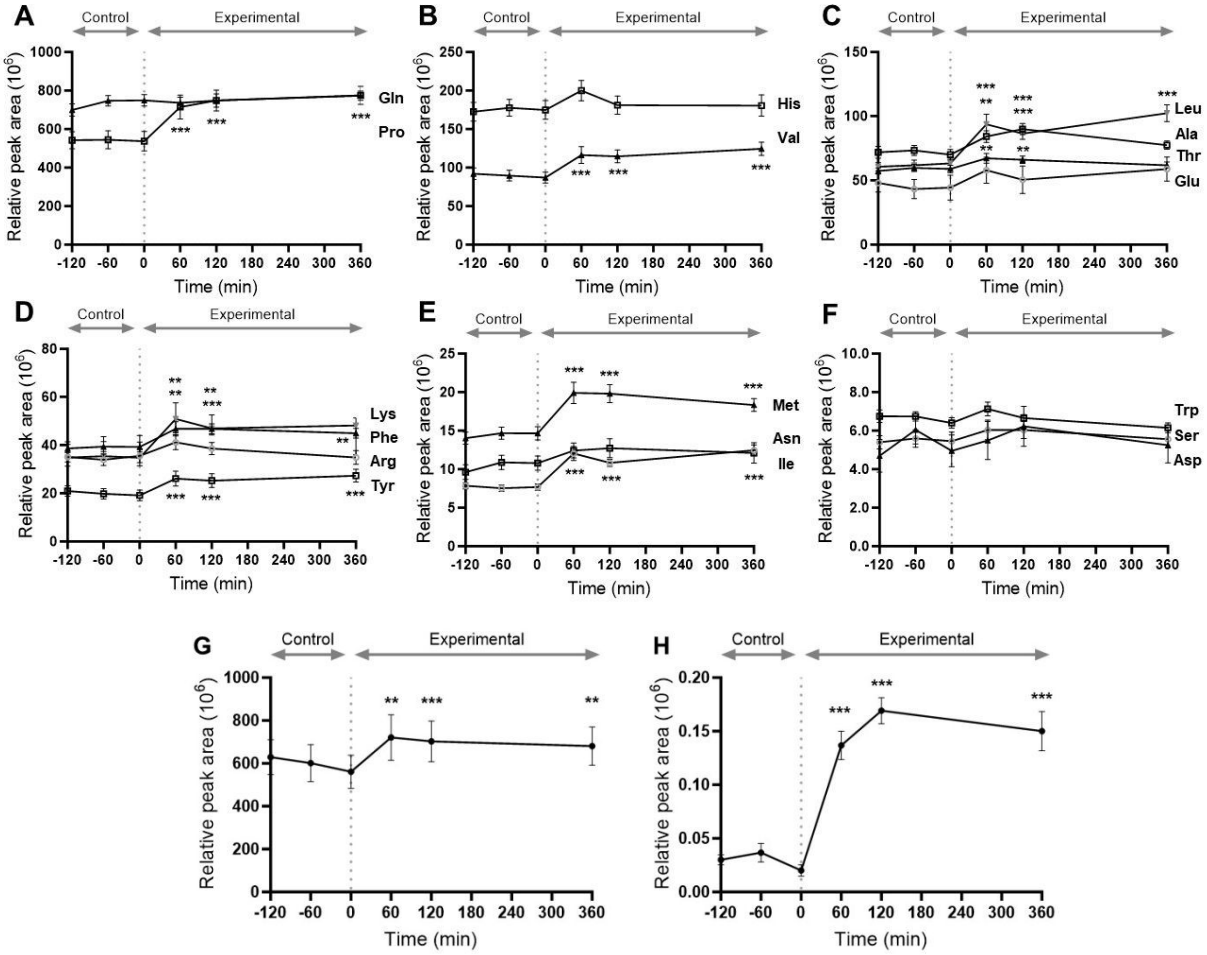

Figure 3.

Open Access Article. Published on 31 March 2026. Downloaded on 4/2/2026 12:19:51 AM.
This article is licensed under a Creative Commons Attribution 3.0 Unported Licence.

Food & Function Accepted Manuscript

View Article Online
DOI: 10.1039/D5FO04456A

Open Access Article. Published on 31 March 2026. Downloaded on 4/2/2026 12:19:51 AM.
This article is licensed under a Creative Commons Attribution 3.0 Unported Licence.

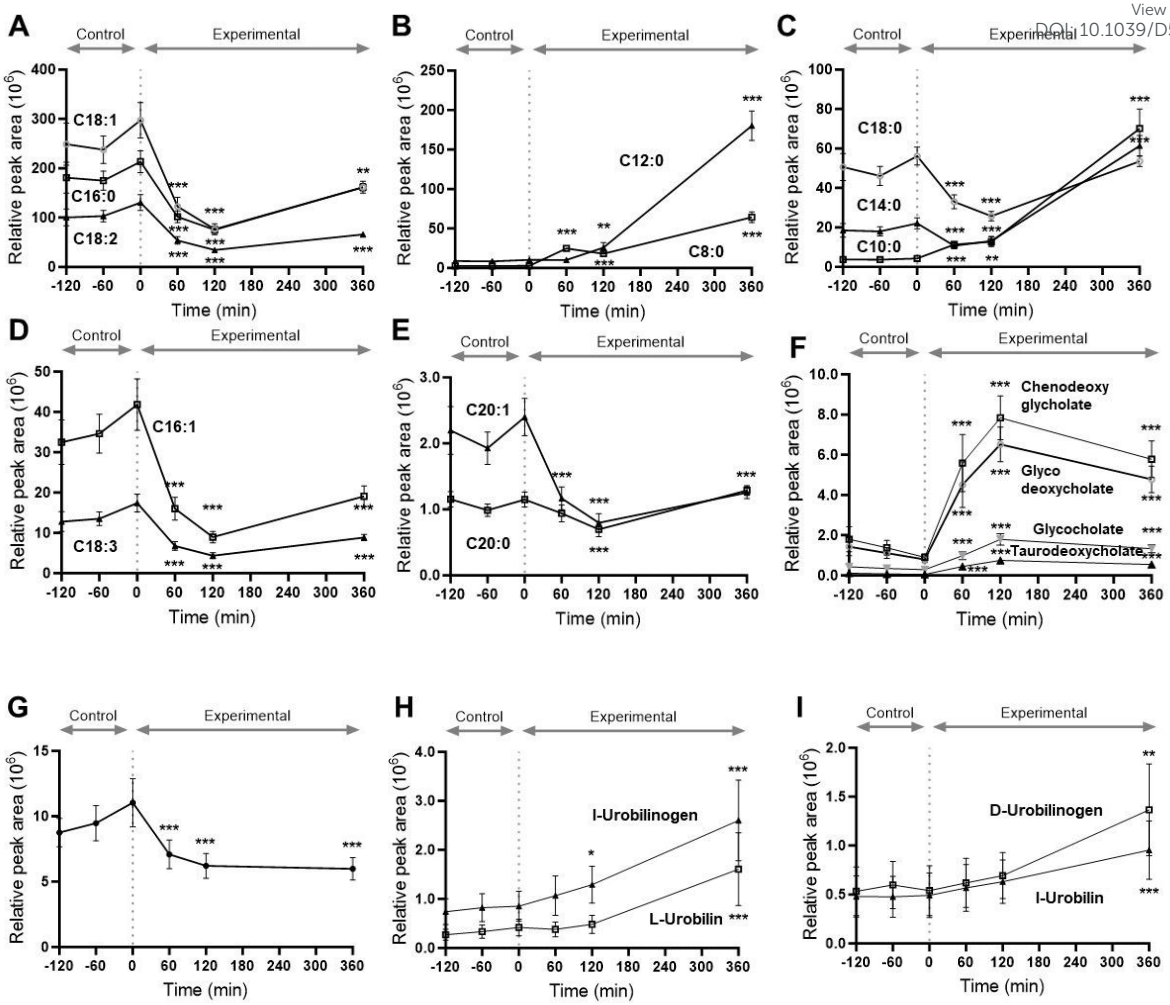

Figure 4.

Food & Function Accepted Manuscript

Open Access Article. Published on 31 March 2026. Downloaded on 4/2/2026 12:19:51
This article is licensed under a Creative Commons Attribution 3.0 Unported

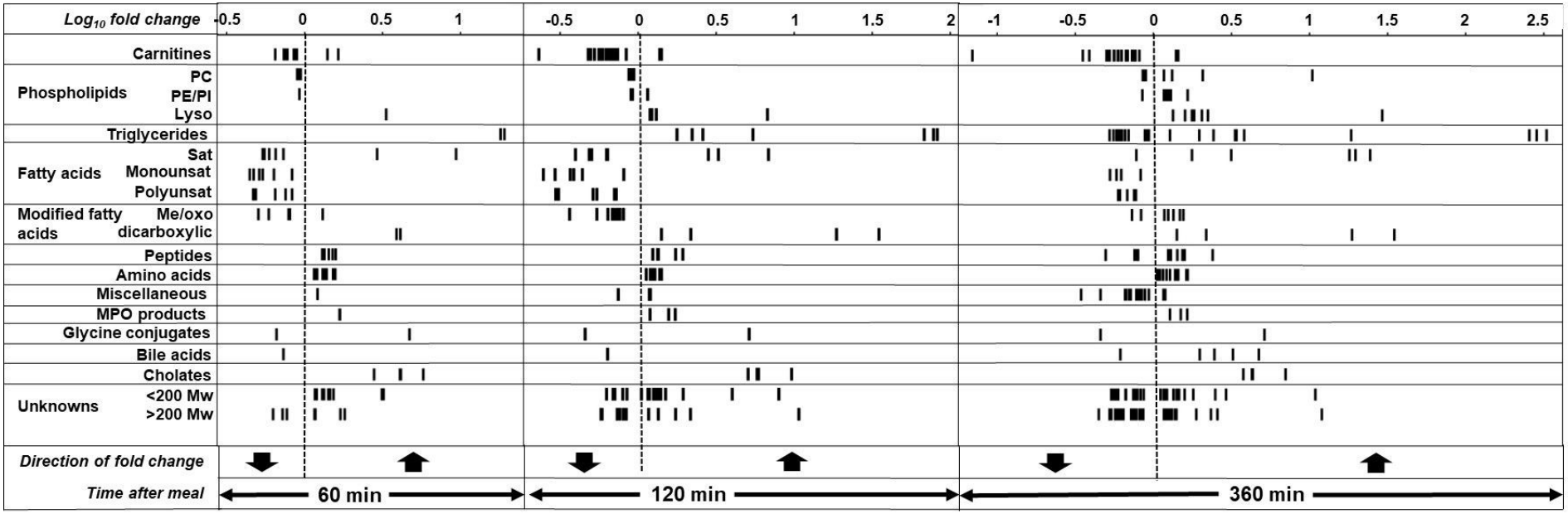

Figure 5.

Food & Function Accepted Manuscript

Open Access Article. Published on 31 March 2026. Downloaded on 4/2/2026 12:19:51
This article is licensed under a Creative Commons Attribution 3.0 Unported
Internal

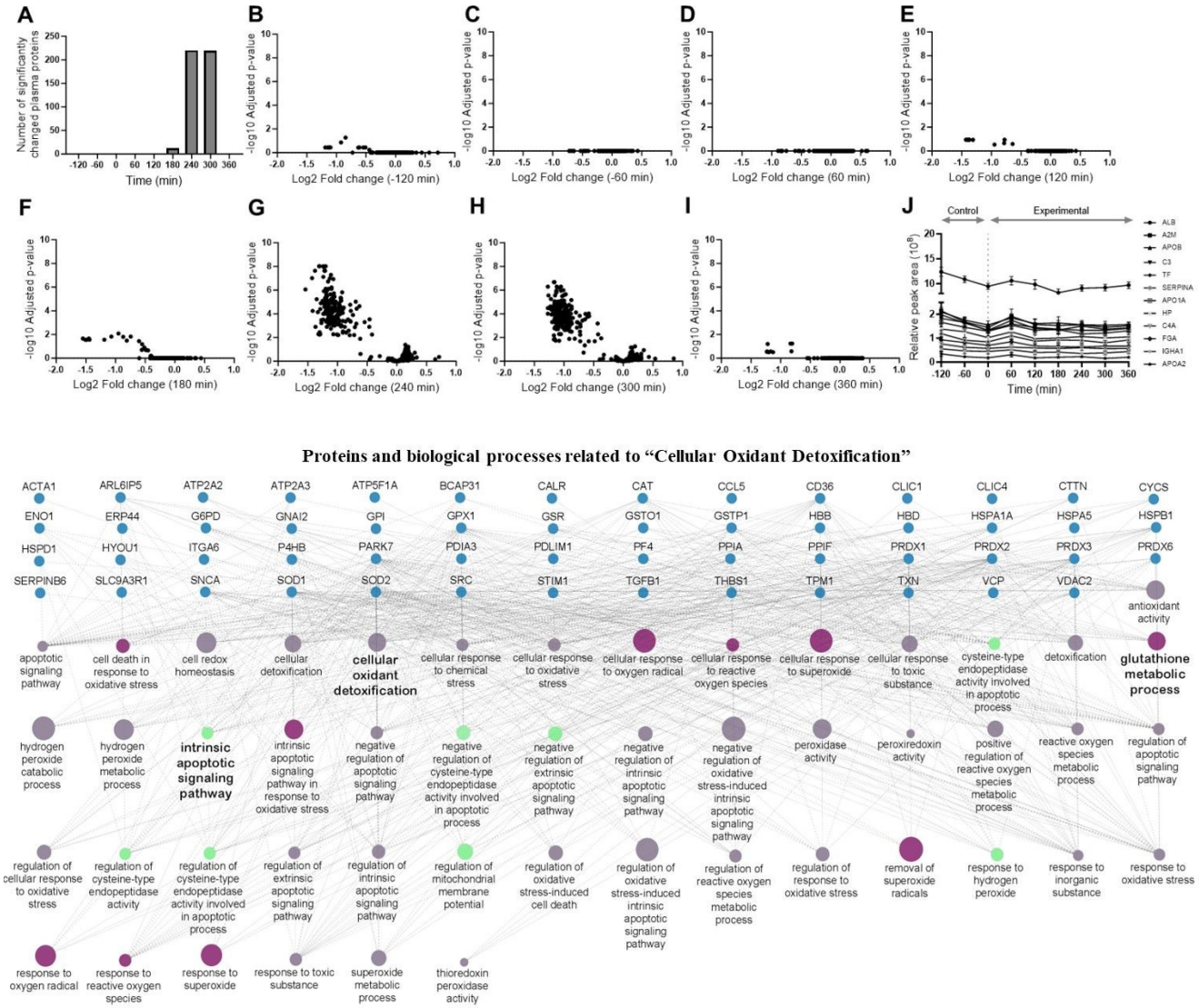

Figure 6.

Food & Function Accepted Manuscript

View Article Online
DOI: 10.1039/D5FO04456A

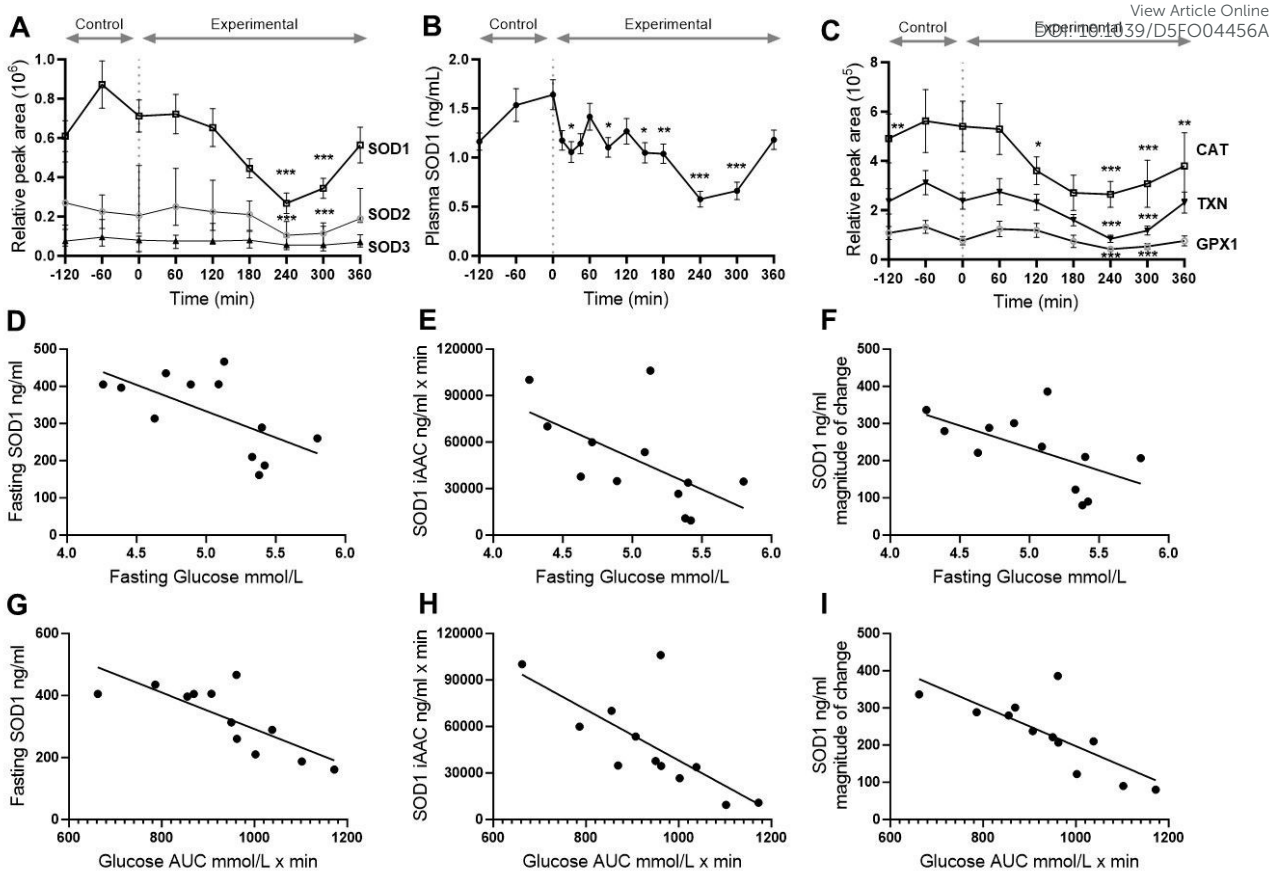

Figure 7.

Open Access Article. Published on 31 March 2026. Downloaded on 4/2/2026 12:19:51 AM.
This article is licensed under a Creative Commons Attribution 3.0 Unported Licence.

Food & Function Accepted Manuscript

View Article Online
DOI: 10.1039/D5FO04456A

Reference list

1. Gearhardt AN, Bueno NB, DiFeliceantonio AG, Roberto CA, Jimenez-Murcia S, Fernandez-Aranda F. Social, clinical, and policy implications of ultra-processed food addiction. BMJ. 2023;383:e075354. doi: 10.1136/bmj-2023-075354.

2. Xourafa G, Korbmacher M, Roden M. Inter-organ crosstalk during development and progression of type 2 diabetes mellitus. Nat Rev Endocrinol. 2024;20(1):27-49. doi: 10.1038/s41574-023-00898-1.

3. Maki KA, Sack MN, Hall KD. Ultra-processed foods: increasing the risk of inflammation and immune dysregulation? Nat Rev Immunol. 2024;24(7):453-4. doi: 10.1038/s41577-024-01049-x.

4. Grinshpan LS, Eilat-Adar S, Ivancovsky-Wajcman D, Kariv R, Gillon-Keren M, Zelber-Sagi S. Ultra-processed food consumption and non-alcoholic fatty liver disease, metabolic syndrome and insulin resistance: A systematic review. JHEP Rep. 2024;6(1):100964. doi: 10.1016/j.jhepr.2023.100964.

5. Mazidi M, Valdes AM, Ordovas JM, Hall WL, Pujol JC, Wolf J, et al. Meal-induced inflammation: postprandial insights from the Personalised REsponses to DIetary Composition Trial (PREDICT) study in 1000 participants. Am J Clin Nutr. 2021;114(3):1028-38. doi: 10.1093/ajcn/nqab132.

6. Zeevi D, Korem T, Zmora N, Israeli D, Rothschild D, Weinberger A, et al. Personalized Nutrition by Prediction of Glycemic Responses. Cell. 2015;163(5):1079-94. doi: 10.1016/j.cell.2015.11.001.

Open Access Article. Published on 31 March 2026. Downloaded on 4/2/2026 12:19:51 AM.
This article is licensed under a Creative Commons Attribution 3.0 Unported Licence.
Food & Function Accepted Manuscript

View Article Online
DOI: 10.1039/D5FO04456A

7. Karimpour M, Surowiec I, Wu J, Gouveia-Figueira S, Pinto R, Trygg J, Zivkovic AM, Nording ML. Postprandial metabolomics: A pilot mass spectrometry and NMR study of the human plasma metabolome in response to a challenge meal. Anal Chim Acta. 2016;908:121-31. doi: 10.1016/j.aca.2015.12.009.

8. Lepine G, Tremblay-Franco M, Bouder S, Dimina L, Fouillet H, Mariotti F, Polakof S. Investigating the Postprandial Metabolome after Challenge Tests to Assess Metabolic Flexibility and Dysregulations Associated with Cardiometabolic Diseases. Nutrients. 2022;14(3). doi: 10.3390/nu14030472.

9. Radjursoga M, Lindqvist HM, Pedersen A, Karlsson BG, Malmodin D, Ellegard L, Winkvist A. Nutritional Metabolomics: Postprandial Response of Meals Relating to Vegan, Lacto-Ovo Vegetarian, and Omnivore Diets. Nutrients. 2018;10(8). doi: 10.3390/nu10081063.

10. Weinisch P, Fiamoncini J, Schranner D, Raffler J, Skurk T, Rist MJ, et al. Dynamic patterns of postprandial metabolic responses to three dietary challenges. Front Nutr. 2022;9:933526. doi: 10.3389/fnut.2022.933526.

11. Blaak EE, Antoine JM, Benton D, Bjorck I, Bozzetto L, Brouns F, et al. Impact of postprandial glycaemia on health and prevention of disease. Obes Rev. 2012;13(10):923-84. doi: 10.1111/j.1467-789X.2012.01011.x.

12. Wright E, Jr., Scism-Bacon JL, Glass LC. Oxidative stress in type 2 diabetes: the role of fasting and postprandial glycaemia. Int J Clin Pract. 2006;60(3):308-14. doi: 10.1111/j.1368-5031.2006.00825.x.

13. Ceriello A, Motz E. Is oxidative stress the pathogenic mechanism underlying insulin resistance, diabetes, and cardiovascular disease? The common soil hypothesis revisited.

Open Access Article. Published on 31 March 2026. Downloaded on 4/2/2026 12:19:51 AM.
This article is licensed under a Creative Commons Attribution 3.0 Unported Licence.
Food & Function Accepted Manuscript

View Article Online
DOI: 10.1039/D5FO04456A

Arterioscler Thromb Vasc Biol. 2004;24(5):816-23. doi: 10.1161/01.ATV.0000122852.22604.78.

14. Sies H, Stahl W, Sevanian A. Nutritional, dietary and postprandial oxidative stress. J Nutr. 2005;135(5):969-72. doi: 135/5/969 [pii].

15. Markey O, McClean CM, Medlow P, Davison GW, Trinick TR, Duly E, Shafat A. Effect of cinnamon on gastric emptying, arterial stiffness, postprandial lipemia, glycemia, and appetite responses to high-fat breakfast. Cardiovasc Diabetol. 2011;10(1):78. doi: 10.1186/1475-2840-10-78.

16. Natella F, Macone A, Ramberti A, Forte M, Mattivi F, Matarese RM, Scaccini C. Red wine prevents the postprandial increase in plasma cholesterol oxidation products: a pilot study. Br J Nutr. 2011;105(12):1718-23. doi: 10.1017/S0007114510005544.

17. Deplanque X, Muscente-Paque D, Chappuis E. Proprietary tomato extract improves metabolic response to high-fat meal in healthy normal weight subjects. Food Nutr Res. 2016;60(1):32537. doi: 10.3402/fnr.v60.32537.

18. Edirisinghe I, Randolph J, Cheema M, Tadapaneni R, Park E, Burton-Freeman B, Kappagoda T. Effect of grape seed extract on postprandial oxidative status and metabolic responses in men and women with the metabolic syndrome - randomized, cross-over, placebo-controlled study. Funct Food Health Dis. 2012;2(12):508-21. doi: DOI 10.31989/ffhd.v2i12.68.

19. Chusak C, Thilavech T, Adisakwattana S. Consumption of Mesona chinensis attenuates postprandial glucose and improves antioxidant status induced by a high carbohydrate meal in overweight subjects. Am J Chin Med. 2014;42(2):315-36. doi: 10.1142/S0192415X14500219.

Open Access Article. Published on 31 March 2026. Downloaded on 4/2/2026 12:19:51 AM.
This article is licensed under a Creative Commons Attribution 3.0 Unported Licence.

Food & Function Accepted Manuscript

View Article Online
DOI: 10.1039/D5FO04456A

20. Denniss SG, Haffner TD, Kroetsch JT, Davidson SR, Rush JW, Hughson RL. Effect of short-term lycopene supplementation and postprandial dyslipidemia on plasma antioxidants and biomarkers of endothelial health in young, healthy individuals. Vasc Health Risk Manag. 2008;4(1):213-22. doi: 10.2147/vhrm.2008.04.01.213.

21. Schindhelm RK, Alssema M, Diamant M, Teerlink T, Dekker JM, Kok A, Kostense PJ, Nijpels G, Heine RJ, Scheffer PG. Comparison of two consecutive fat-rich and carbohydrate-rich meals on postprandial myeloperoxidase response in women with and without type 2 diabetes mellitus. Metabolism. 2008;57(2):262-7. doi: 10.1016/j.metabol.2007.09.010.

22. Metzig AM, Schwarzenberg SJ, Fox CK, Deering MM, Nathan BM, Kelly AS. Postprandial endothelial function, inflammation, and oxidative stress in obese children and adolescents. Obesity (Silver Spring). 2011;19(6):1279-83. doi: 10.1038/oby.2010.318.

23. Nolfi-Donegan D, Braganza A, Shiva S. Mitochondrial electron transport chain: Oxidative phosphorylation, oxidant production, and methods of measurement. Redox Biol. 2020;37:101674. doi: 10.1016/j.redox.2020.101674.

24. Du XL, Edelstein D, Rossetti L, Fantus IG, Goldberg H, Ziyadeh F, Wu J, Brownlee M. Hyperglycemia-induced mitochondrial superoxide overproduction activates the hexosamine pathway and induces plasminogen activator inhibitor-1 expression by increasing Sp1 glycosylation. Proc Natl Acad Sci U S A. 2000;97(22):12222-6. doi: 10.1073/pnas.97.22.12222.

25. Du X, Matsumura T, Edelstein D, Rossetti L, Zsengeller Z, Szabo C, Brownlee M. Inhibition of GAPDH activity by poly(ADP-ribose) polymerase activates three major

Open Access Article. Published on 31 March 2026. Downloaded on 4/2/2026 12:19:51 AM.
This article is licensed under a Creative Commons Attribution 3.0 Unported Licence.
Food & Function Accepted Manuscript

View Article Online
DOI: 10.1039/D5FO04456A

941 pathways of hyperglycemic damage in endothelial cells. J Clin Invest. 2003;112(7):1049-57.
942 doi: 10.1172/JCI18127.

943 26. Brownlee M. Biochemistry and molecular cell biology of diabetic complications.
944 Nature. 2001;414(6865):813-20. doi: 10.1038/414813a.

945 27. Heden TD, Liu Y, Sims LJ, Whaley-Connell AT, Chockalingam A, Dellsperger KC,
946 Kanaley JA. Meal frequency differentially alters postprandial triacylglycerol and insulin
947 concentrations in obese women. Obesity (Silver Spring). 2013;21(1):123-9. doi:
948 10.1002/oby.20247.

949 28. Lacroix S, Des Rosiers C, Gayda M, Nozza A, Thorin E, Tardif JC, Nigam A. A
950 single Mediterranean meal does not impair postprandial flow-mediated dilatation in healthy
951 men with subclinical metabolic dysregulations. Appl Physiol Nutr Metab. 2016;41(8):888-94.
952 doi: 10.1139/apnm-2015-0490.

953 29. Metzig AM, Schwarzenberg SJ, Fox CK, Deering MM, Nathan BM, Kelly AS.
954 Postprandial endothelial function, inflammation, and oxidative stress in obese children and
955 adolescents. Obesity. 2011;19(6):1279-83. doi: 10.1038/oby.2010.318.

956 30. Serviddio G, Loverro G, Vicino M, Prigigallo F, Grattagliano I, Altomare E,
957 Vendemiale G. Modulation of endometrial redox balance during the menstrual cycle: relation
958 with sex hormones. J Clin Endocrinol Metab. 2002;87(6):2843-8. doi:
959 10.1210/jcem.87.6.8543.

960 31. Tirimacco R SP, Siew L, Cowley PJ, Tideman PA. *Evaluation of the HemoCue WBC*
961 *Diff point of care instrument* [Internet]. Bedford Park, SA, Australia, Integrated
962 Cardiovascular Clinical Network CHSA; Available from:
963 http://www.aacb.asn.au/documents/item/1004.

Open Access Article. Published on 31 March 2026. Downloaded on 4/2/2026 12:19:51 AM.
This article is licensed under a Creative Commons Attribution 3.0 Unported Licence.

Food & Function Accepted Manuscript

View Article Online
DOI: 10.1039/D5FO04456A

964 32. Knopp JL, Holder-Pearson L, Chase JG. Insulin Units and Conversion Factors: A
965 Story of Truth, Boots, and Faster Half-Truths. J Diabetes Sci Technol. 2019;13(3):597-600.
966 doi: 10.1177/1932296818805074.

967 33. Stoessel DN, C.J.; Jones, A.J.;Ferrins, L.;Ellis, K.M.; Riley, J.;Rahmani, R.;Read,
968 K.D.;McConville, M.J.;Avery, V.M.;Baell, J.B.;Creek, D.J. Metabolomics and lipidomics
969 reveal perturbation of sphingolipid metabolism by a novel anti-trypanosomal 3-(oxazolo[4,5-
970 b]pyridine-2-yl)anilide. Metabolomics. 2016;12:126. doi: 10.1007/s11306-016-1062-1.

971 34. Creek DJ, Jankevics A, Breitling R, Watson DG, Barrett MP, Burgess KE. Toward
972 global metabolomics analysis with hydrophilic interaction liquid chromatography-mass
973 spectrometry: improved metabolite identification by retention time prediction. Anal Chem.
974 2011;83(22):8703-10. doi: 10.1021/ac2021823.

975 35. Chambers MC, Maclean B, Burke R, Amodei D, Ruderman DL, Neumann S, et al. A
976 cross-platform toolkit for mass spectrometry and proteomics. Nat Biotechnol.
977 2012;30(10):918-20. doi: 10.1038/nbt.2377.

978 36. Creek DJ, Jankevics A, Burgess KE, Breitling R, Barrett MP. IDEOM: an Excel
979 interface for analysis of LC-MS-based metabolomics data. Bioinformatics. 2012;28(7):1048-
980 9. doi: 10.1093/bioinformatics/bts069.

981 37. Scheltema RA, Jankevics A, Jansen RC, Swertz MA, Breitling R. PeakML/mzMatch:
982 a file format, Java library, R library, and tool-chain for mass spectrometry data analysis. Anal
983 Chem. 2011;83(7):2786-93. doi: 10.1021/ac2000994.

984 38. Barber E, Houghton MJ, Visvanathan R, Williamson G. Measuring key human
985 carbohydrate digestive enzyme activities using high-performance anion-exchange

Open Access Article. Published on 31 March 2026. Downloaded on 4/2/2026 12:19:51 AM.
This article is licensed under a Creative Commons Attribution 3.0 Unported Licence.

Food & Function Accepted Manuscript

View Article Online
DOI: 10.1039/D5FO04456A

986 chromatography with pulsed amperometric detection. Nat Protoc. 2022;17(12):2882-919. doi:
987 10.1038/s41596-022-00736-0.

988 39. Bindea G, Mlecnik B, Hackl H, Charoentong P, Tosolini M, Kirilovsky A, Fridman
989 WH, Pages F, Trajanoski Z, Galon J. ClueGO: a Cytoscape plug-in to decipher functionally
990 grouped gene ontology and pathway annotation networks. Bioinformatics. 2009;25(8):1091-
991 3. doi: 10.1093/bioinformatics/btp101.

992 40. Shannon P, Markiel A, Ozier O, Baliga NS, Wang JT, Ramage D, Amin N,
993 Schwikowski B, Ideker T. Cytoscape: a software environment for integrated models of
994 biomolecular interaction networks. Genome Res. 2003;13(11):2498-504. doi:
995 10.1101/gr.1239303.

996 41. Benson TW, Weintraub NL, Kim HW, Seigler N, Kumar S, Pye J, et al. A single
997 high-fat meal provokes pathological erythrocyte remodeling and increases myeloperoxidase
998 levels: implications for acute coronary syndrome. Lab Invest. 2018;98(10):1300-10. doi:
999 10.1038/s41374-018-0038-3.

1000 42. Frijhoff J, Winyard PG, Zarkovic N, Davies SS, Stocker R, Cheng D, et al. Clinical
1001 Relevance of Biomarkers of Oxidative Stress. Antioxid Redox Signal. 2015;23(14):1144-70.
1002 doi: 10.1089/ars.2015.6317.

1003 43. Tsan MF. Myeloperoxidase-mediated oxidation of methionine. J Cell Physiol.
1004 1982;111(1):49-54. doi: 10.1002/jcp.1041110109.

1005 44. Yu PH, Bailey BA. New sensitive high-performance liquid chromatographic method
1006 for p-tyrosine aminotransferase assay. J Chromatogr. 1986;362(1):55-9. doi: 10.1016/s0021-
1007 9673(01)86950-8.

Open Access Article. Published on 31 March 2026. Downloaded on 4/2/2026 12:19:51 AM.
This article is licensed under a Creative Commons Attribution 3.0 Unported Licence.

Food & Function Accepted Manuscript

View Article Online
DOI: 10.1039/D5FO04456A

1008 45. Turunen S, Huhtakangas J, Nousiainen T, Valkealahti M, Melkko J, Risteli J,
1009 Lehenkari P. Rheumatoid arthritis antigens homocitrulline and citrulline are generated by
1010 local myeloperoxidase and peptidyl arginine deiminases 2, 3 and 4 in rheumatoid nodule and
1011 synovial tissue. Arthritis Res Ther. 2016;18(1):239. doi: 10.1186/s13075-016-1140-9.

1012 46. Maiocchi SL, Ku J, Thai T, Chan E, Rees MD, Thomas SR. Myeloperoxidase: A
1013 versatile mediator of endothelial dysfunction and therapeutic target during cardiovascular
1014 disease. Pharmacol Ther. 2021;221:107711. doi: 10.1016/j.pharmthera.2020.107711.

1015 47. Anderson NL, Anderson NG. The human plasma proteome: history, character, and
1016 diagnostic prospects. Mol Cell Proteomics. 2002;1(11):845-67. doi: 10.1074/mcp.r200007-
1017 mcp200.

1018 48. Gordin D, Saraheimo M, Tuomikangas J, Soro-Paavonen A, Forsblom C, Paavonen
1019 K, et al. Influence of Postprandial Hyperglycemic Conditions on Arterial Stiffness in Patients
1020 With Type 2 Diabetes. J Clin Endocrinol Metab. 2016;101(3):1134-43. doi: 10.1210/jc.2015-
1021 3635.

1022 49. Malinska H, Kahleova H, Topolcan O, Vrzalova J, Oliyarnyk O, Kazdova L, Belinova
1023 L, Hill M, Pelikanova T. Postprandial oxidative stress and gastrointestinal hormones: is there
1024 a link? PLoS One. 2014;9(8):e103565. doi: 10.1371/journal.pone.0103565.

1025 50. Saxena R, Madhu SV, Shukla R, Prabhu KM, Gambhir JK. Postprandial
1026 hypertriglyceridemia and oxidative stress in patients of type 2 diabetes mellitus with
1027 macrovascular complications. Clinica Chimica Acta. 2005;359(1-2):101-8. doi:
1028 10.1016/j.cccn.2005.03.036.

Open Access Article. Published on 31 March 2026. Downloaded on 4/2/2026 12:19:51 AM.
This article is licensed under a Creative Commons Attribution 3.0 Unported Licence.

Food & Function Accepted Manuscript

View Article Online
DOI: 10.1039/D5FO04456A

51. Canale RE, Farney TM, McCarthy CG, Bloomer RJ. Influence of acute exercise of varying intensity and duration on postprandial oxidative stress. Eur J Appl Physiol. 2014;114(9):1913-24. doi: 10.1007/s00421-014-2912-z.

52. Faraci FM, Didion SP. Vascular Protection. Arterioscler Thromb Vasc Biol. 2004;24(8):1367-73. doi: doi:10.1161/01.ATV.0000133604.20182.cf.

53. Guo J, Liu H, Zhao D, Pan C, Jin X, Hu Y, Gao X, Rao P, Liu S. Glucose-lowering effects of orally administered superoxide dismutase in type 2 diabetic model rats. NPJ Sci Food. 2022;6(1):36. doi: 10.1038/s41538-022-00151-5.

54. Mathew M, Tay E, Cusi K. Elevated plasma free fatty acids increase cardiovascular risk by inducing plasma biomarkers of endothelial activation, myeloperoxidase and PAI-1 in healthy subjects. Cardiovascular Diabetology. 2010;9(1):9. doi: 10.1186/1475-2840-9-9.

55. Baldus S, Eiserich JP, Mani A, Castro L, Figueroa M, Chumley P, et al. Endothelial transcytosis of myeloperoxidase confers specificity to vascular ECM proteins as targets of tyrosine nitration. J Clin Invest. 2001;108(12):1759-70. doi: 10.1172/JCI12617.

56. Eiserich JP, Baldus S, Brennan ML, Ma W, Zhang C, Tousson A, et al. Myeloperoxidase, a leukocyte-derived vascular NO oxidase. Science. 2002;296(5577):2391-4. doi: 10.1126/science.1106830.

57. Tyagi A, Kumar U, Santosh VS, Reddy S, Mohammed SB, Ibrahim A. Partial replacement of dietary linoleic acid with long chain n-3 polyunsaturated fatty acids protects against dextran sulfate sodium-induced colitis in rats. Prostaglandins Leukot Essent Fatty Acids. 2014;91(6):289-97. doi: 10.1016/j.plefa.2014.09.003.

Open Access Article. Published on 31 March 2026. Downloaded on 4/2/2026 12:19:51 AM.
This article is licensed under a Creative Commons Attribution 3.0 Unported Licence.
Food & Function Accepted Manuscript

View Article Online
DOI: 10.1039/D5FO04456A

58. Mi Y, Chin YX, Cao WX, Chang YG, Lim PE, Xue CH, Tang QJ. Native kappa-carrageenan induced-colitis is related to host intestinal microecology. Int J Biol Macromol. 2020;147:284-94. doi: 10.1016/j.ijbiomac.2020.01.072.

59. Ostojic SM. Plasma creatine as a marker of mitochondrial dysfunction. Med Hypotheses. 2018;113:52-3. doi: 10.1016/j.mehy.2018.02.022.

60. Doessegger L, Schmitt G, Lenz B, Fischer H, Schlotterbeck G, Atzpodien EA, et al. Increased levels of urinary phenylacetylglycine associated with mitochondrial toxicity in a model of drug-induced phospholipidosis. Ther Adv Drug Saf. 2013;4(3):101-14. doi: 10.1177/2042098613479393.

61. Guasch-Ferre M, Hruby A, Toledo E, Clish CB, Martinez-Gonzalez MA, Salas-Salvado J, Hu FB. Metabolomics in Prediabetes and Diabetes: A Systematic Review and Meta-analysis. Diabetes Care. 2016;39(5):833-46. doi: 10.2337/dc15-2251.

62. Xu G, Hansen JS, Zhao XJ, Chen S, Hoene M, Wang XL, et al. Liver and Muscle Contribute Differently to the Plasma Acylcarnitine Pool During Fasting and Exercise in Humans. J Clin Endocrinol Metab. 2016;101(12):5044-52. doi: 10.1210/jc.2016-1859.

63. Dordevic AL, Williamson G. Systematic Review and Quantitative Data Synthesis of Peripheral Blood Mononuclear Cell Transcriptomics Reveals Consensus Gene Expression Changes in Response to a High Fat Meal. Mol Nutr Food Res. 2023;67(23):e2300512. doi: 10.1002/mnfr.202300512.

64. Nakeeb AP, H.A. Pathophysiology of biliary tract obstruction. Edtion ed. In: Blumgart LH, ed. Surgery of the Liver, Biliary Tract and Pancreas: Elsevier, 2006:79-97.

Open Access Article. Published on 31 March 2026. Downloaded on 4/2/2026 12:19:51 AM.
This article is licensed under a Creative Commons Attribution 3.0 Unported Licence.
Food & Function Accepted Manuscript

View Article Online
DOI: 10.1039/D5FO04456A

1071 65. Liang X, Wang R, Luo H, Liao Y, Chen X, Xiao X, Li L. The interplay between the
1072 gut microbiota and metabolism during the third trimester of pregnancy. Front Microbiol.
1073 2022;13:1059227. doi: 10.3389/fmicb.2022.1059227.

1074 66. Brüll V, Burak C, Stoffel-Wagner B, Wolffram S, Nickenig G, Müller C, et al. Acute
1075 intake of quercetin from onion skin extract does not influence postprandial blood pressure
1076 and endothelial function in overweight-to-obese adults with hypertension: a randomized,
1077 double-blind, placebo-controlled, crossover trial. Eur J Nutr. 2017;56(3):1347-57. doi:
1078 https://doi.org/10.1007/s00394-016-1185-1.

1079 67. Carnevale R, Silvestri R, Loffredo L, Novo M, Cammisotto V, Castellani V,
1080 Bartimoccia S, Nocella C, Violi F. Oleuropein, a component of extra virgin olive oil, lowers
1081 postprandial glycaemia in healthy subjects. Br J Clin Pharmacol. 2018;84(7):1566-74. doi:
1082 10.1111/bcp.13589.

1083 68. Murray M, Selby-Pham S, Colton B-L, Bennett L, Williamson G, Dordevic AL. Does
1084 timing of phytonutrient intake influence the suppression of postprandial oxidative stress? A
1085 systematic literature review. Redox Biol. 2021;46:102123. doi:
1086 https://doi.org/10.1016/j.redox.2021.102123.

1087 69. Ghanim H, Sia CL, Korzeniewski K, Lohano T, Abuaysheh S, Marumganti A,
1088 Chaudhuri A, Dandona P. A resveratrol and polyphenol preparation suppresses oxidative and
1089 inflammatory stress response to a high-fat, high-carbohydrate meal. J Clin Endocrinol Metab.
1090 2011;96(5):1409-14. doi: 10.1210/jc.2010-1812.

1091

Open Access Article. Published on 31 March 2026. Downloaded on 4/2/2026 12:19:51 AM.
This article is licensed under a Creative Commons Attribution 3.0 Unported Licence.
Food & Function Accepted Manuscript

View Article Online
DOI: 10.1039/D3FO04456A

Acute response to a high-fat-high-refined carbohydrate meal in healthy young men shows novel perturbation of multiple metabolic and defense pathways

Aimee L Dordevic [1, 2*] aimee.dordevic@monash.edu, ORCID 0000-0002-0405-3164

Margaret Murray [1, 3, 4] msmurray@swin.edu.au, ORCID 0000-0003-3767-6947

Michael J Houghton [1,2] michael.houghton@monash.edu, ORCID 0000-0001-6579-7995

Nina M Trinquet [1,2] nina.trinquet1@monash.edu, ORCID 0009-0009-2828-2963

Nicole J Kellow [1,2] nicole.kellow@monash.edu, ORCID 0000-0002-4511-7259

Ralf B Schittenhelm [5] ralf.schittenhelm@monash.edu, ORCID 0000-0001-8738-1878

Christopher K Barlow [5] chris.barlow@monash.edu, ORCID 0000-0001-9309-2829

Kaitlin Day [6] kaitlin.day@kcl.ac.uk, ORCID 0000-0003-3846-8568

Louise Bennett [3] louise.bennett1@monash.edu, ORCID 0000-0001-9421-4410

Beau-Luke Colton [1] beau.colton@gmail.com

Gary Williamson [1,2,7] g.williamson@qub.ac.uk, ORCID 0000-0002-5624-6267

Open Access Article. Published on 31 March 2026. Downloaded on 4/2/2026 12:19:51 AM.
This article is licensed under a Creative Commons Attribution 3.0 Unported Licence.

Food & Function Accepted Manuscript

Data availability

The metabolomics data have been submitted to the Metabolights platform (https://www.ebi.ac.uk/metabolights/) with the dataset identifier MTBLS10972. *The data will be made available following publication.*

The mass spectrometry proteomics data have been deposited to the ProteomeXchange Consortium via the PRIDE partner repository (https://www.ebi.ac.uk/pride/) with the dataset identifier PXD055358. *Before publication, the data are only available to reviewers: Username: reviewer_pxd055358@ebi.ac.uk; Password: BMzRoQsEgAg4. The data will be made publicly available on publication of this work.*